Water Research 308 (2027) 126999

Contents lists available at ScienceDirect

Water Research

journal homepage: www.elsevier.com/locate/watres

Residence times of English estuaries

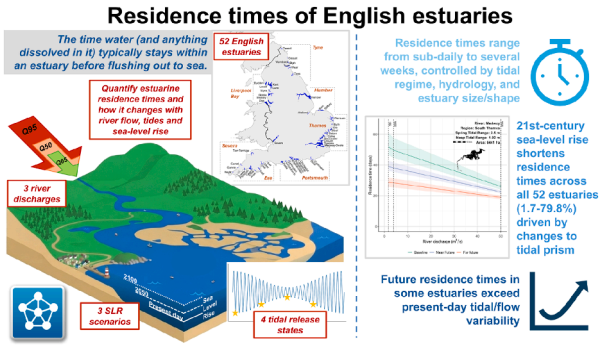
Thomas W. Clough [a], Charlotte Lyddon [b], Aaron Furnish [a], Mirko Barada [b], Tom Coulthard [c], Andy Barkwith [f], Fai Fung [e], Gemma Coxon [d], Laura Devitt [d], Davey L. Jones [g], Nick Hayes [h], Alec Hutchings [h], Harriet G. Orr [h], Peter Robins [a,*]

[a] School of Ocean Sciences, Bangor University, Marine Centre Wales, Menai Bridge, LL59 5AB, UK
[b] School of Environmental Sciences, University of Liverpool, Liverpool, L69 3GP, UK
[c] Department of Natural Sciences, Manchester Metropolitan University, Manchester, M15 6BX, UK
[d] School of Geographical Sciences, University of Bristol, Bristol, BS8 1SS, UK
[e] UK Met Office, Exeter, EX1 3PB, UK
[f] British Geological Survey, Keyworth, Nottingham, NG12 5GG, UK
[g] School of Environmental and Natural Sciences, Bangor University, Bangor, LL57 2UW, UK
[h] The Environment Agency, Bristol, BS15AH, UK

HIGHLIGHTS

- Residence time modelled in 52 English estuaries under tides, flow and sea-level rise.
- Residence times vary from sub-daily to weeks with size, shape, tides and flow.
- 21st century sea-level rise reduces residence times by 1.7-79.8%.
- Future residence times in some estuaries exceed present-day tidal/flow variability.

GRAPHICAL ABSTRACT



ARTICLE INFO

Keywords:
Residence time
Climate change
Sea-level rise
Water quality
Pollution
Modelling
Flushing time

ABSTRACT

The residence time of estuaries is a fundamental indicator of biogeochemical cycling, ecological productivity, pollution, and human health risk. Residence times of UK estuaries are estimated to vary from days to weeks, depending on tidal and riverine variability, as well as estuary size and shape; yet are largely unquantified for present-day and future climate conditions. This study presents the first national-scale modelling assessment of residence times across 52 English estuaries, using a consistent framework of high-resolution bathymetry and hydrodynamic modelling (Delft3D-FM). Simulations were run under present-day conditions and projected sea-level anomalies for 2050 and 2100, based on UK Climate Projections 2018 Representative Concentration Pathway 8.5 scenarios. Residence times were estimated using conservative tracer decay, across a range of river flow and tidal conditions. Results demonstrate substantial inter-estuary and intra-estuary variability, with present-day mean residence times ranging from <1 day in small, well-flushed estuaries to ~100 days in microtidal or volumetrically large estuaries. Tidal flux, river inflow, and estuary size/shape emerged as dominant

* Corresponding author.
E-mail address: p.robins@bangor.ac.uk (P. Robins).

https://doi.org/10.1016/j.watres.2026.126999
Received 9 June 2026; Received in revised form 18 August 2026; Accepted 20 September 2026
Available online 21 September 2026
0043-1354/© 2026 The Authors. Published by Elsevier Ltd. This is an open access article under the CC BY license (http://creativecommons.org/licenses/by/4.0/).

controls on flushing behaviour, allowing classification of estuary residence times as either tidally or fluvially dominated. Under projected sea-level rise (SLR) scenarios, residence times decreased in all estuaries due to the increased tidal prism and reduced intertidal storage. In four estuaries (Plymouth Sound, Portsmouth Harbour, Southampton Water, and Ore), SLR-driven changes exceeded present-day natural variability, suggesting a step-change in hydrodynamic functioning. This work provides critical evidence for climate adaptation planning in estuarine and coastal environments and a scalable framework to identify systems where future changes in residence time may compromise water quality objectives.

1. Introduction

Estuaries are critical transition zones where fluvial and marine fluxes converge, driving hydrodynamic, sedimentary, and biogeochemical processes that vary within and between different estuary types, and over a range of temporal scales (Kennish, 2002; Bianchi, 2007). Among the suite of metrics used to characterise estuarine behaviour, residence time – also commonly called flushing time – occupies a central role in governing nutrient cycling, contaminant dispersion, and ecological productivity (Valle-Levinson, 2010; MacCready et al., 2021). Here we define residence time as the elapsed duration (e-folding decay time) required for water or dissolved or neutrally-buoyant material suspended within it to be exported from the estuary. In simple terms, residence time reflects how long water and anything dissolved within it (e.g., nutrients, sediments, pollutants) physically remains within an estuary before being flushed out to sea. A glossary defining key technical terms used throughout this study is presented in Supplementary Table S0. Long residence times, e.g., several weeks, can promote stratification, reduce oxygen replenishment, retain pollutants, and foster conditions conducive to eutrophication and the development of harmful algal blooms (Cloern and Jassby, 2010). Conversely, shorter residence times of a few days typically enhance flushing efficiency, dilute pollutant concentrations, and support robust trophic exchanges (Honti et al., 2010). With the continued influx of nutrients and pollutants to estuaries, and growing concern over potential increases in harmful contaminant concentrations under a changing climate (Nedwell et al., 2002; Robins et al. 2016), it is important to quantify spatio-temporal variability of estuarine residence times and predict changes in response to projected climate change. In the UK, such an analysis has not previously been undertaken at national scale. This gap undermines adaptive management strategies, because without understanding residence time, managers cannot accurately predict pollutant flushing, nutrient cycling, or ecosystem responses to stressors. Hence, efforts to preserve water quality and long-term ecosystem resilience into the future are hindered (Nicholls and Cazenave, 2010; Legg, 2021).

Future trajectories of sea-level rise (SLR), altered storm and precipitation patterns, and land-use change will collectively reshape estuaries and change their retention potential (Robins et al., 2016; Du et al., 2018; Palmer et al., 2019). Numerical studies have demonstrated that even modest increases in mean sea level can modulate tidal propagation and resonance, alter intertidal inundation patterns, and shift the balance between advective and diffusive transport, thereby exerting non-linear effects on residence times (Pugh and Woodworth, 2014). For instance, Irby et al. (2018) reported that a 0.5 m SLR in Chesapeake Bay reduced residence times by approximately 20% due to the enhanced tidal prism, whereas in more weakly tidal basins, the same SLR extended residence time by up to 15% through increased stratification. In the Oosterschelde, Netherlands, SLR amplified tidal range and shortened water renewal times (Jiang et al., 2020), while in the Gironde, France, it altered the position of the turbidity maximum alongside seasonal variations in river inflow (van Maanen and Sottolichio, 2018). Such shifts in flushing and inundation can cause direct water-quality consequences, including the remobilisation of contaminants stored in estuarine sediments (Kerl et al., 2023). Such differing responses highlight that tidal flux, hydrology, and estuary size/shape collectively determine estuary residence times (Ranjbar et al., 2020).

Historically, idealised models and scaling analyses have provided first-order estimates of estuarine flushing dynamics (Fischer et al., 1979; Lukitina 1998; Zimmerman, 2018), yet they inherently lack spatial resolution (e.g., do not account for estuary shape or bathymetric features, or within-estuary circulation and mixing behaviour) and assume riverine, tidal, and mixing conditions do not change during the period of flushing; for UK estuaries, these assumptions may not be valid (Lyddon et al. 2023). To improve on these first-order estimates, hydrodynamic models have been used to simulate estuarine hydrodynamics with high fidelity (Iglesias et al., 2019). Yuan et al. (2007) modelled the Mersey Estuary (UK) using a numerical hydrodynamic–dispersion model and reported residence times of 1–4 days, though the structured mesh approach employed poorly resolved the small-scale hydrodynamic features of the estuary (Mora-Uribe et al., 2025). Huggett et al. (2021) applied an unstructured mesh model coupled with a particle tracking model to simulate Christchurch Harbour, showing residence times to vary from <1 day to >20 days depending on river flow.

Estuaries are ubiquitous coastal features (estimates range from 1200 to 4400 estuaries worldwide depending on the definition; Bianchi et al., 2007) but exhibit pronounced heterogeneity in geomorphology, tidal regime, hydrology, and anthropogenic influence. In the UK, to date there has been no coherent suite of high-resolution models spanning the full diversity of estuarine systems. Previous studies of residence time have focused on single or small clusters of estuaries – for example, Vermeulen (2003) investigated sediment-transport in the Humber estuary within a Delft3D framework – while broader assessments have relied on either coarse regional models (Čož et al., 2017) or simplified box representations (Gillibrand et al., 2013) that cannot resolve sub-kilometric features critical for residence-time estimation (MacCready et al., 2021). Given that English estuaries range from macrotidal, funnel-shaped systems (e.g., Severn, Humber) to microtidal lagoons (e.g., Poole Harbour, Langstone Harbour), and from polymodal river networks (e.g., Thames) to tide-dominated deltas (e.g., Deben), a comprehensive, multi-estuary modelling assessment of residence times will establish a baseline against which future changes can be systematically evaluated.

The present study addresses this gap by constructing and validating a suite of Delft3D Flexible Mesh models covering the majority (52) of English estuaries (Fig. 1). Estuaries were selected on the basis of the availability of UK Water Framework Directive (WFD) Cycle 2 Transitional Water Body polygons (EA, 2015), together with corresponding river gauge monitoring records, ensuring a consistent national modelling framework (Supplementary Table S1). The overall aim is twofold: first, to characterise baseline residence times across a spectrum of morphological and hydrodynamic contexts; and second, to quantify how projected annual SLR under the Representative Concentration Pathway 8.5 (RCP8.5) scenario for near future (in 2050) and far future (in 2100) will alter flushing dynamics. By applying a uniform modelling framework encompassing consistent boundary forcing, mesh design principles, and tracer-release protocols, this work facilitates direct comparability between estuaries and isolates the role of inherent geomorphic and hydrodynamic variability. With coastal populations in England expected to grow by 10–20% over the next three decades (Hall et al., 2006), understanding how SLR changes will impact estuarine flushing is critical for long-term infrastructure planning, flood risk mitigation, and biodiversity preservation (Khojasteh et al., 2020).

2. Methods

The hydrodynamic simulations were conducted using the Delft3D Flexible Mesh Suite (Van Gent, 2014). The Delft3D system is partially open source: the numerical codebase is available publicly (https://oss.deltares.nl/web/delft3d/get-started), whereas the graphical user interface (GUI), including the mesh generation software, remains proprietary. The model's flexible mesh architecture and robust wetting and drying algorithms make it particularly well-suited for coastal and estuarine water quality assessments involving intertidal processes (e.g., Mendes et al., 2021; Bai et al., 2022). Unlike traditional structured grids which represent the coastline as a fixed lattice of rectangular cells, an unstructured grid can vary in shape and resolution across the model domain. This allows the mesh to follow complex, irregular estuary boundaries and channels closely, while concentrating resolution in narrow or morphologically complex areas without the prohibitive

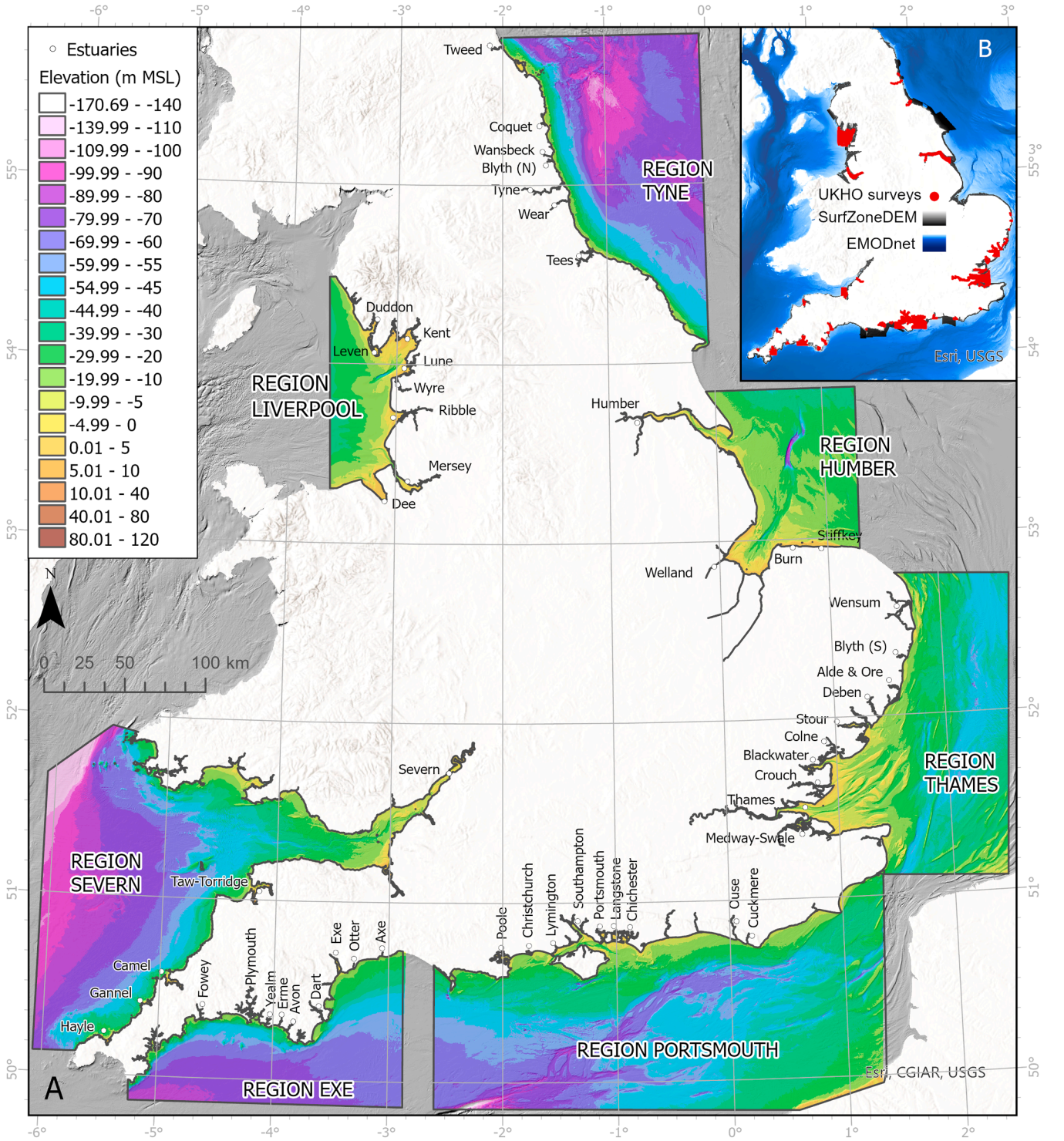


Fig. 1. (A) Map showing the 52 estuaries in England analysed in this study, and final 20 m DEMs segmented into seven regions (coloured areas)[1]; (B) Bathymetry data sources.

[1]DEMs were built only for selected areas – estuarine regions, while gaps between regions are filled with 100 m EMODnet DEM (grey shaded DEM).

computational cost of applying that resolution uniformly across an entire regional domain. Delft3D-FM has been applied widely to estuarine environments: For example, Pannozzo et al. (2021) examined salt-marsh resilience under combined SLR and increased storm intensity of the Ribble estuary, England; Yang et al. (2022) quantified sediment transport pathways in the Pearl River estuary, and Wang et al. (2022) evaluated flushing dynamics under extreme river floods in the Yangtze estuary.

The D-Flow FM module solves the depth-averaged (2D) or fully three-dimensional shallow water equations for momentum and continuity using a finite-volume numerical scheme (see Supplementary Info S1). A comprehensive formulation of these equations is presented in Van Gent (2014). For this study, D-Flow FM was dynamically coupled with the D-Water Quality module to simulate conservative tracer transport (see Section 2.1.2). Simulations were executed in parallel on Bangor University's high-performance computing infrastructure (https://www.supercomputing.wales/), enabling computationally efficient regional-scale modelling.

Seven regional Delft3D-FM model domains were constructed to simulate hydrodynamics across 52 English estuaries, with unstructured meshes refined to ~3 m resolution within estuaries and bathymetry derived from a hierarchy of national datasets referenced to Mean Sea Level. Models were validated against tide gauge records (RMSE 0.591 ± 0.29 m across all domains) and salinity observations (RMSE 2.9 psu in Liverpool Bay), with additional independent validation in the Conwy estuary (RMSE 1.73–3.74 psu). Full details of mesh configuration, DEM construction, parameterisation, and validation are provided in the Supplementary Material (S1-S4). Supplementary Material S4 provides the corresponding time series comparisons and domain statistical breakdowns. Direct field validation of residence time itself (e.g., dye release or drifter tracking) was not feasible at the scale of 52 estuaries and remains a priority for future work.

2.1. Idealised estuary residence time simulations

2.1.1. Hydrodynamic simulations (using **D**-Flow)

For each of the seven regional models, we applied D-Flow to simulate the 2D hydrodynamics (including salinity) of each estuary, covering a present-day two-month period, following a three-month spin-up period to reach steady-state salinity conditions – i.e., when sufficient time has been modelled such that inputs and outputs are reflecting natural processes, rather than recovering from perturbations derived from initial conditions of the models. For the present-day simulations, offshore boundary forcing comprised the principal semi-diurnal lunar (M2) and solar (S2) tidal constituents only. We intentionally limited the tidal forcing to M2 and S2 (i.e., neglecting other tidal constituents such as K1, O1, P1, N2, and M4) so that the (idealised) elevations broadly represented mean spring-neap tidal cycles. Tidal forcing data were sourced from the TPXO global tidal model (Egbert et al., 1994) at 0.25° resolution and interpolated to model boundary nodes. Salinity at the tidal boundary was applied as a constant forcing (34 ppt). Riverine forcing was applied as constant discharge rates at each river inflow boundary location, using flow magnitudes representative of 5th, 50th, and 95th percentile conditions (See Supplementary Table S1) derived from 30-year observational records for each river (01 January 1984 to 31 December 2013) (Lyddon et al., 2023).

Projected future changes in mean sea level were simulated within the hydrodynamic models, forced with UKCP18 (UK Climate Projections 2018) RCP (Representative Concentration Pathway) −8.5 SLR projections for 2050 and 2100 (Met Office, 2018; UKCP18). The RCP-8.5 scenario represents a high-emissions, plausible "worst-case" pathway that, although is considered unlikely by some studies (e.g., Scafetta, 2024), remains widely used for stress-testing coastal systems under significant climate pressure (Jevrejeva et al., 2023). Testing estuaries against a plausible upper bound of SLR identifies which systems are most sensitive under stress, providing a conservative basis for prioritising conservation and management efforts; a sensitivity potentially missed by a mid- or low-range SLR scenarios. Data was provided on a 12 km resolution coastal grid around the UK, for 12 ensemble simulations – the 50th percentile values were chosen to reflect the mean of the ensemble range, consistent with current UK national guidance. For 2050, SLR projections were between 0.24 m and 0.31 m, depending on region, and for 2100 between 0.66 and 0.81 m (See Supplementary Table S2). For river boundary forcing, historical flow percentiles were applied, meaning that these simulations isolated the effects of SLR without incorporating projected changes in river discharge.

2.1.2. 1Residence time simulations (using **D**-Water quality)

The D-Water Quality module was applied in offline mode (i.e. driven by the pre-computed hydrodynamics from D-Flow described in Section 2.1.1) to simulate conservative tracer transport from within each estuary. The tracer was initially distributed uniformly within each estuary domain polygon. Four simulations were performed whereby the tracers were introduced at different stages of the spring-neap tidal cycle: (1) spring tide; (2) mid spring-to-neap tide; (3) neap tide; and (4) mid neap-to-spring tide. For each case, tracers were released at low tide. These simulations were repeated for all river flow (5th/50th/95th percentile; Section 2.1.1) and SLR scenarios, totalling 1872 residence time simulations (3 river flows × 4 release times × 3 sea levels × 52 estuaries).

For each simulation, the dispersal and dilution of the tracer was simulated over space and time to estimate the residence times of the tracers. The time-dependent, estuary-averaged concentration $\overline{C}(t)$, as a percentage of the initial tracer concentration $\overline{C}(0)$, was calculated with a 12.5-h moving mean applied to remove tidal oscillations. Residence time (T_R) was defined as the elapsed time required for the area-averaged concentration to decline to 37% of its initial value:

$$T_R = \min\{t | \overline{C}(t) \leq 0.37\,\overline{C}(0)\}$$

This definition corresponds to the e-folding time of tracer mass decay, consistent with established residence time methodologies (Zimmerman, 1976; Monsen et al., 2002). This approach quantifies the advection, diffusion, and dilution processes that determine estuarine flushing efficiency and pollutant retention.

Unless otherwise stated, "mean residence time" refers to the value simulated at median river discharge (Q50), averaged across the four tidal release states (spring, mid spring-to-neap, neap, and mid neap-to-spring). Where distributions or ranges are reported, these span all twelve baseline tidal/flow combinations.

For each estuary i, residence time was simulated for every combination of river flow q {Q5, Q50, Q95} and tracer release state s {spring, mid spring-to-neap, neap, mid neap-to-spring}, giving twelve baseline values $T_R(i, q, s)$.

The variability attributable to tidal state was defined as the maximum range across release states, evaluated at each flow and taking the largest:

$$\Delta T_{\text{tide}}(i) = \max_q[\max_s T_R(i, q, s) - \min_s T_R(i, q, s)$$

The variability attributable to river flow was defined equivalently, as the maximum range across flows evaluated at each release state:

$$\Delta T_{\text{flow}}(i) = \max_s[\max_q T_R(i, q, s) - \min_q T_R(i, q, s)$$

Estuaries were classified as fluvially dominated where $\Delta T_{\text{flow}} > \Delta T_{\text{tide}}$ (above the 1:1 line) and tidally dominated where $\Delta T_{\text{tide}} > \Delta T_{\text{flow}}$ (below it). The 1:1 line therefore represents equal sensitivity to both forcings, and perpendicular distance from it indicates the strength of dominance. Note that this classification describes the *relative sensitivity* of each estuary to tidal versus fluvial forcing, not the absolute magnitude of its residence time; a rapidly flushing estuary and a highly retentive one may share the same classification.

2.1.3. Sensitivity of residence time to changes in hydrology and stratification

Since the model scenarios above were forced with temporally constant 5th/50th/95th percentile river flow forcing, we performed additional simulations with the Liverpool Bay regional model forced with realistic temporally variable (15-minute resolution) river flow data to more accurately reproduce short-term hydrodynamic variability and freshwater pulses (see Supplementary Material, Fig. S4). The simulation period (10–23 January 2014) coincided with exceptionally wet conditions (Met Office, 2014), allowing model performance to be evaluated under high-flow, storm-influenced conditions representative of extreme winter hydrology.

Further sensitivity tests explored the effects of stratification on residence times: comparing depth-averaged simulations with 3D simulations (see Supplementary Material, Fig. S1.1). These simulations were performed for the Liverpool Bay regional domain, where the 2D and 3D residence time simulations produced very similar outputs, inferring that the depth-averaged approach was feasible for this region where the macrotidal and hypertidal regimes generally result in well-mixed waters (Polton et al. 2011). Although much of the English coast experiences a macrotidal regime (Robins et al. 2015), there are some estuaries where weaker tidal forcing and relatively high freshwater input can promote stratification. To identify any partially-mixed estuaries, a stratification index $R = Q(T/2)/V$ was applied to all 52 estuaries for three flow scenarios (Q5, Q50, Q95), where Q is river discharge (m^3/s), T is the M2 tidal period (44,712 s), V is the tidal prism estimated as the product of estuary surface area and mean tidal range (m^3). $R > 1$ indicates conditions conducive to stratification (Supplementary Table S3). Only the Tweed estuary exceeded the stratification threshold, and only under high flow conditions (Q95; $R = 1.48$); all other estuaries remained well-mixed across all flow scenarios. The 2D-3D comparison of the Liverpool Bay domain confirms that the depth averaged approach performs well where estuaries are well mixed, consistent with the stratification index results for this region ($R < 1$ under all conditions tested). However, this comparison does not independently verify model performance under stratified conditions ($R > 1$). Therefore, the Tweed estuary under Q95 flow may be biased by the 2D assumption and should be treated with more caution than the rest of the dataset.

3. Results

3.1. Baseline estuary residence times

Estuarine residence times, simulated throughout a mean spring-neap tidal cycle, and for 5th/50th/95th percentile river flows representative of the baseline period 1980 - 2000, are shown in Fig. 2, for a subset of four English estuaries: the Severn, Mersey, Dee and Tyne. Simulated baseline residence times for all 52 estuaries are provided in the Supplementary Material, Figs. S5–S12. Under these baseline forcing conditions, residence times for each estuary exhibited considerable temporal variability driven by estuary-specific tidal and river forcing (described in Section 3.1.1), as well as intra-estuary variability in mean residence times due to differing estuary volumes and shapes (described in 3.1.2).

Residence times ranged from less than one day in small, well-flushed systems (e.g., Stiffkey, 0.16 days; Erme, 0.30 days; Tweed, 0.47 days) to several weeks in larger, more retentive estuaries such as the Medway (42.5 days), Blyth (41.0 days), and Wensum (38.6 days). The Ore estuary (southeast England) exhibited by far the longest mean residence time of 109.5 days (range: 89.8–126.8 days across tidal and flow scenarios), more than double that of the next longest estuary. This is attributed to the highly restricted tidal inlet formed by the Orford Ness shingle spit, which severely limits exchange with the open coast, combined with a low tidal range (~1 m) and small catchment area. The Stiffkey estuary exhibited the shortest mean residence time of 0.16 days (~4 h), with negligible sensitivity to river discharge variability (±0 days) and minimal sensitivity to tidal forcing (±0.17 days), reflecting its small size and open tidal exchange.

3.1.1. Temporal variability in baseline residence times

Estuary residence times varied (or did not) with increasing river flow forcing, i.e., the larger gradients of the curves in Fig. 2 indicated more riverine sensitivity (e.g., Figs. 2a, d). For most estuaries, increasing river flow, from low (5th percentile) to high (95th percentile) values, resulted in notable reductions in residence time, e.g., by 52.9 days (92%; Wensum), 28.8 days (80%; Severn), and 37.5 days (69%; Blyth (Suffolk)). In contrast, the residence times of other systems such as the Crouch (26%; 6.2 days reduction), Poole Harbour (27%; 4.8 days), Southampton Water (28%; 9.8 days), and Portsmouth Harbour (29%; 5.2 days) were relatively insensitive to fluvial variability (i.e., the curves in Fig. 2c which resemble near-horizontal lines), indicating that the contribution of the riverine flux to the flushing of these estuary types was relatively small.

The baseline residence times also varied depending on when the tracer was released within the spring-neap tidal cycle (i.e., the thicker vertical shading in Fig. 2 indicates more tidal sensitivity). Most estuaries experience considerable variability in tidal volume flux over the spring-neap cycle (e.g., Robins et al. 2015) and, hence, the tracer release timing did influence residence times. Generally, tracers released during neap tides or mid spring-to-neap tides (i.e., reduced tidal exchange during the initial days after release, and shown as red and blue curves in Fig. 3) resulted in longer residence times than tracers released during spring tides or neap-to-spring tides (green and yellow curves in Fig. 2).

Tidal sensitivity varied considerably across the 52 estuaries, with a national mean of 3.54 days. The greatest tidal sensitivity was found in the Medway (12.9 days; neap RT: 57.5 days vs. spring RT: 44.6 days; mean tidal range: 1.92 m; volume: 2.21×10^8 m^3) and Thames (12.7 days; neap RT: 41.1 days vs. spring RT: 28.4 days; mean tidal range: 1.90 m; volume: 1.58×10^9 m^3), both large, tidally-energetic southeast England estuaries. At the other extreme, the Axe, Otter, and Wansbeck exhibited zero tidal sensitivity (mean tidal ranges: 1.81, 1.88, and 1.18 m; volumes: 4.5×10^5, 6.9×10^5, and 1.2×10^6 m^3 respectively), where residence times were identical regardless of spring or neap release.

The variability in residence times due to tidal and river flow forcing, expressed as the coefficient of variation (CV), defined as the ratio of the standard deviation to the mean, ranged from 0.11 to 1.26 across the 52 estuaries, with a national mean CV of 0.46 (median: 0.43), indicating substantial intra-estuary variability in the sensitivity of each estuary to different tidal/fluvial conditions.

The baseline residence times can therefore be classified according to whether their temporal variability is driven primarily by river flow or tidal dynamics, or by both in similar proportions. This classification is shown in Fig. 3, which plots the relative contribution of tidal versus fluvial variability in residence time for all estuaries. Estuaries plotted above the diagonal dashed line are classified as fluvially-dominated, whereas those below the line as tidally-dominated. For example, the Wensum estuary (eastern England, volume = 3.43×10^7 m^3) is fluvially-dominated: the residence time varied by several weeks due to river flow variability (5th/95th percentile flows = 1.64/76.0 m^3/s), but the tidal cycle had only a minor influence (spring/neap tidal range = 0.93/0.51m; tidal variability 3.2 days). For fluvially-dominated estuaries, the range of variability tended to be greater under low-flow scenarios, rather than median or high flows, suggesting that low fluvial input becomes a limiting factor for estuary flushing.

Tidally-dominated estuaries are strongly influenced by the spring–neap tidal cycle (See Supplementary Figure S13), which governs changes in the tidal prism and, consequently, flushing efficiency. For example, the Ouse estuary (southeast England, volume = 1.95×10^6 m^3) is tidally-dominated: the residence time varied by approximately 11 days depending on when within the spring-neap tidal cycle the tracer was released (spring/neap tidal range = 1.89/0.73 m), but varied by only ~1 day due to river flow changes (5th/95th percentile

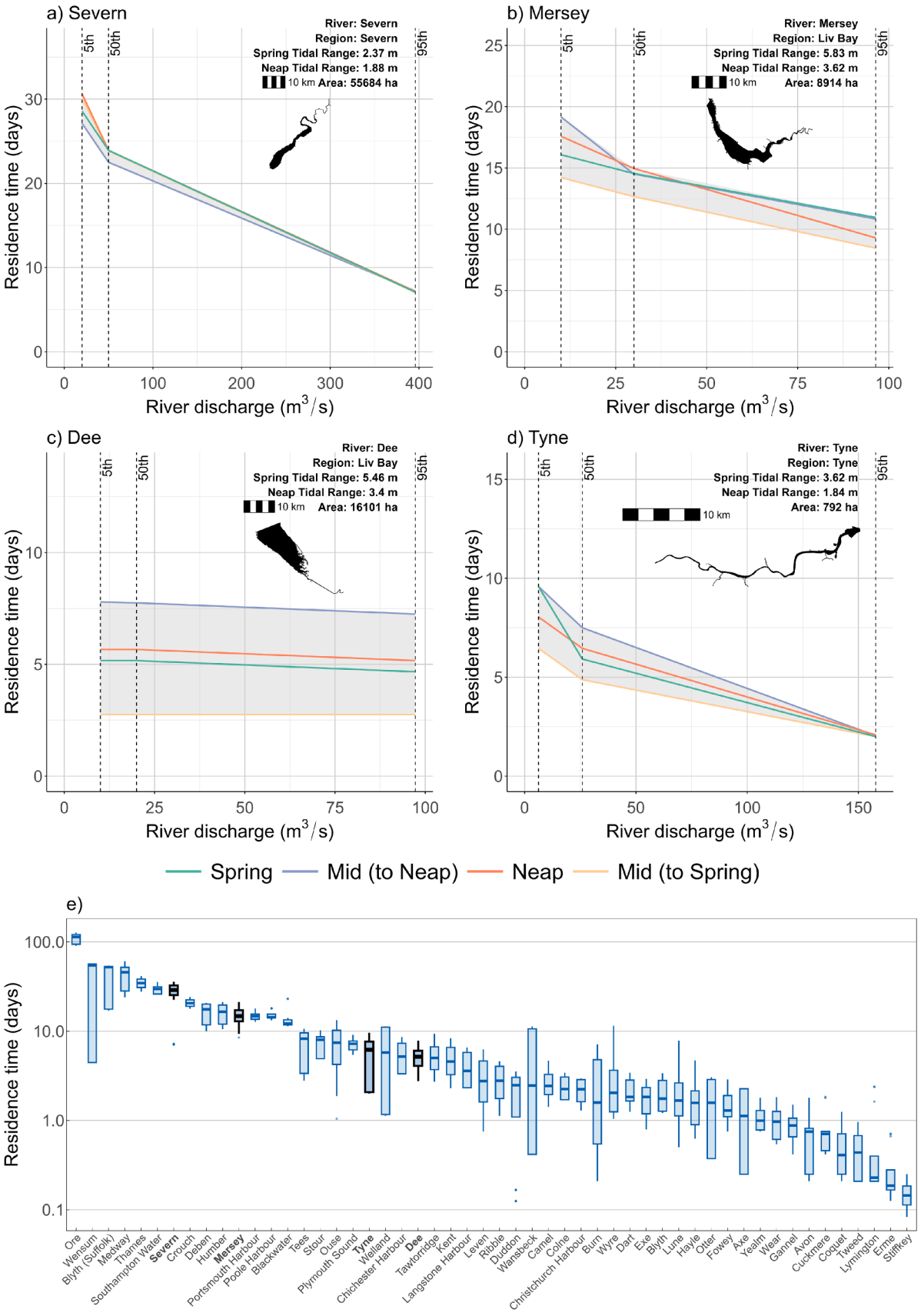


Fig. 2. Simulated baseline residence times for four representative estuaries (a–d) as a function of river discharge (x-axis) and tidal state (shading; four curves represent release timing within the spring-neap cycle). Insets show estuary shape, area, and tidal regime. (e) Ranked residence times across all 52 estuaries; boxes show interquartile range, whiskers show full range, dots show outliers. Y-axis is log-scaled (days).

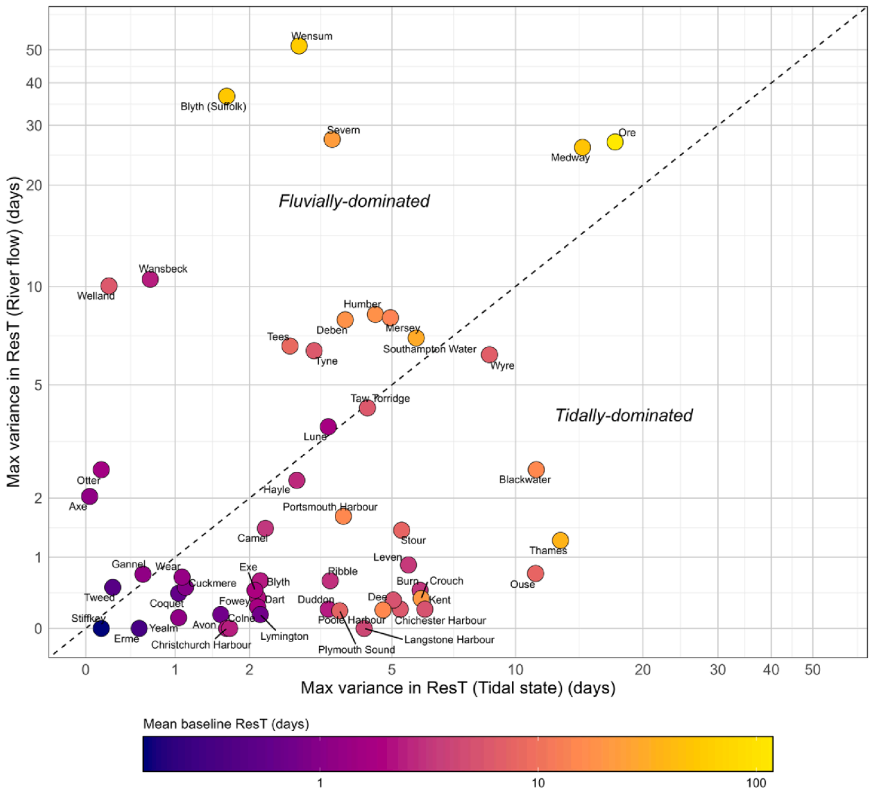


Fig. 3. Characterisation of 52 estuaries by the dominant driver of residence time variability under baseline conditions. Axes show the maximum range in residence time attributable to tidal state (x, ΔT_{tide}) and river flow (y, ΔT_{flow}), as defined in Section 2.1.2. Estuaries below the dashed diagonal are tidally dominated; those above are fluvially dominated. Points are coloured by mean baseline residence time (days; Q50, averaged across the four tidal release states). Axes show the maximum range in residence time attributable to tidal state (x) and river flow (y).

flows = 0.26/8.08 m^3/s).

3.1.2. *Intra-estuary variability in baseline residence time due to estuary volume and shape*

The specific physical size and shape of each estuary further control its residence time. For the Severn and Humber – two of the largest estuaries in England (each ~300 km^2) – we simulated prolonged residence times (mean = 27.31 and 16.16 days respectively; Fig. 4), despite strong advective flushing potential from their macrotidal/hypertidal regimes (spring tidal range = 10.5 m and 5.8 m) and relatively high fluvial inflows (50 and 60 m^3/s). In these systems, the large estuarine volume is the dominant factor constraining tracer flushing. In contrast, there were eleven estuaries with an area <2 km^2 (Otter, Cuckmere, Coquet, Axe, Wansbeck, Gannel, Ouse, Erme, Blyth, Welland, and Tweed). These varied considerably in residence time (0.3–7.8 days), reflecting the influence of other controlling factors even at small scales. Notably, the Ouse (1.24 km^2) and the Welland (1.77 km^2) exhibit relatively long residence times of 7.8 and 5.8 days respectively, attributable to their microtidal regimes (spring tidal range of <1 m) and very low freshwater inflows (<2 m^3/s).

There are 38 intermediately sized estuaries (2 – 160 km^2) with mean residence times varying between 0.16 and 118 days. For these systems, estuary shape becomes an important control on residence times. The Mersey is an intermediate sized estuary (~90 km^2) which also exhibited relatively long residence times of the order of several weeks. This is primarily attributed to its shape, which promotes retention, being relatively long (>40 km) and meandering with a narrow mouth cross-section (1.5 km^2), despite large tidal (spring tidal range = 8.3 m) and riverine fluxes (~30 m^3/s). In contrast, the Dee estuary (~161 km^2), which is larger than the Mersey with a comparable tidal regime (spring tidal range = 4.4 m) and similar freshwater input (~20 m^3/s), exhibited a mean residence time of only 5.3 days. The Dee's substantially wider mouth (8.7 km) and shorter channel length (31 km) facilitate more efficient tidal flushing, reducing residence times despite the larger estuarine volume.

3.2. *Influence of sea-level rise on residence times*

Changes in estuarine residence times under future sea-level rise (SLR) was evaluated for UKCP18 RCP8.5 projections corresponding to the years 2050 and 2100. Results for four representative estuaries (Severn, Mersey, Dee, and Tyne) are presented in Fig. 5, while the results for all 52 estuaries simulated are provided in the Supplementary Material Figures S14–S21.

Simulations revealed a general trend of decreasing residence times with increasing sea level. The magnitude of change varied considerably between estuaries, reflecting differences in morphology, tidal regime, and baseline residence time. For example, in the Ribble estuary, the mean residence time (2.93 days under baseline conditions) halved to 1.45 days by 2050, and approximately halved again by 2100 (SLR of 0.66 m), to 0.75 days; 73.4% reduction from the baseline. In the Mersey estuary, mean residence times reduced at a lesser rate – from ~15 days (baseline), by ~26% to 11 days (2050), and by ~47% to 8 days (2100).

The largest reductions were observed in smaller, tidally-dominated estuaries with relatively simple morphologies. The Burn estuary experienced the greatest proportional decline, with mean residence time reducing from 2.91 days (baseline) to 1.14 days by 2050 (−61.0%) and 0.59 days by 2100 (−79.8%). Similarly, the Fowey (−77.5%), Ribble (−74.1%), Blyth (−72.2%), and Duddon (−67.3%) estuaries all exhibited reductions exceeding 65% by 2100. In contrast, the smallest responses to SLR were found in estuaries with very low baseline tidal forcing or restricted exchange with the open coast. The Ouse estuary exhibited a reduction of 1.7% by 2100 (7.43 to 7.30 days), while Stiffkey (−4.4%), Welland (−14.4%), Otter (−19.7%), and Axe (−20.5%) also

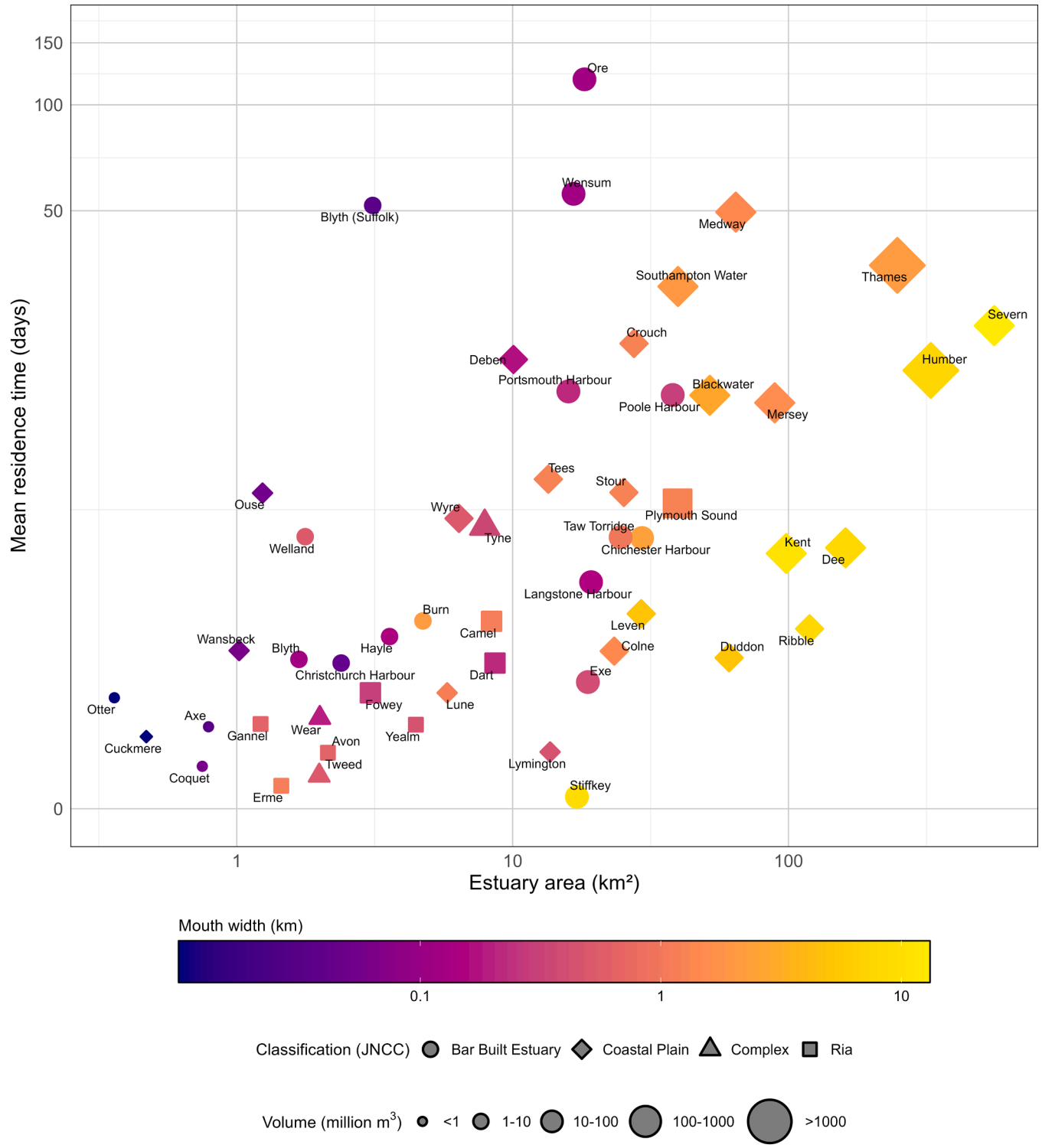


Fig. 4. Mean baseline residence time (Q50, averaged across the four tidal release states) as a function of estuary area for 52 English estuaries. Point colour indicates estuary mouth width (km), shape indicates JNCC geomorphological classification, and point size indicates estuarine volume (million m^3). Both axes are log-scaled; the y-axis uses a pseudo-log transformation to accommodate near-zero values.

showed comparatively modest responses.

Fig. 6a illustrates the spatial distribution of mean residence times for all 52 estuaries under baseline conditions. Fig. 6b presents the projected changes (reductions) in these mean residence times under the 2100 SLR scenario. Fig. 6c presents box-and-whisker plots of the median and interquartile range of residence times for each estuary for the baseline, 2050 SLR, and 2100 SLR scenarios – the estuaries are ranked so that those most sensitive to future residence time changes are clear.

Across the 52 estuaries, median residence times decreased from 2.82 days (baseline) to 1.49 days (2100 SLR), with maxima falling from 126.79 days to 84.58 days (Ore estuary) and minima remained effectively unchanged at 0.08 days (Stiffkey estuary). The Ore exhibited the largest absolute decline, with its median residence time decreasing from 113.54 to 64.31 days between baseline and 2100 SLR (a reduction of

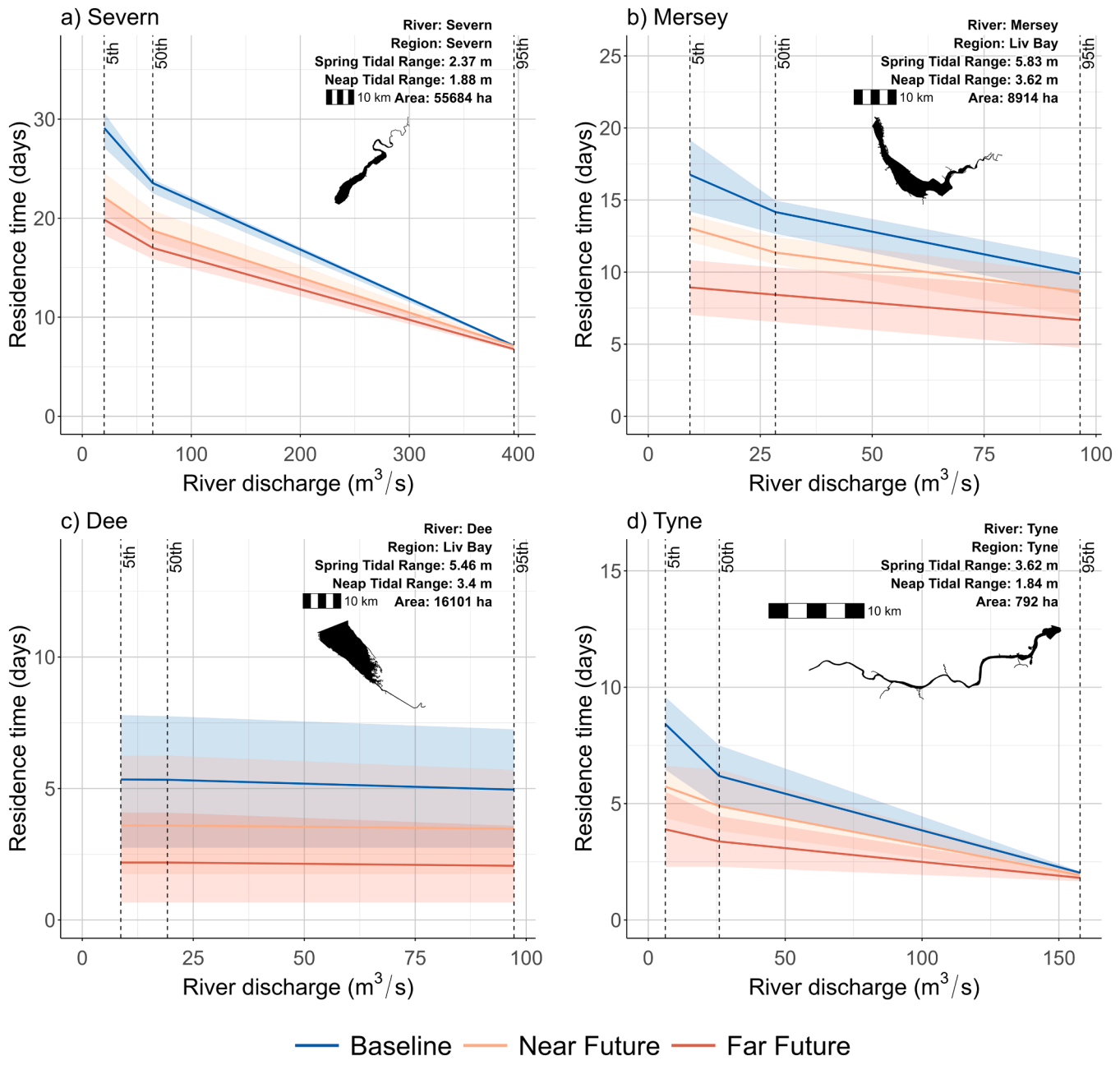


Fig. 5. Simulated residence times for four estuaries under baseline (blue), near-future 2050 (orange), and far-future 2100 (red) RCP8.5 SLR scenarios, as a function of river discharge (x-axis) and tidal state (shaded bands). Dashed vertical lines indicate 5th, 50th, and 95th percentile baseline flows. Insets show estuary shape and area.

49.23 days). By contrast, the Ribble and Blyth estuaries demonstrated the strongest proportional reductions, with medians falling from 2.79 to 0.63 days (77.42% reduction) and 1.75 to 0.25 days (85.71% reduction), respectively.

These reductions in residence times can be attributed to increased volume exchange per tidal cycle, i.e., an increased tidal prism, in response to sea-level rise. As an example, Fig. 7 summarises the hydrodynamic metrics controlling residence time for the Ribble estuary. The tidal prism increased non-linearly with cross-sectional area at the estuary mouth through the spring-neap tidal cycle, with ranges of 20–41 million m^3 (baseline), 25–47 million m^3 (2050 SLR), and 33–64 million m^3 (2100 SLR) (Fig. 7a). Ebb tidal fluxes (Q_{out}) increased with sea level rise from 745/227 m^3/s (median/interquartile range) under baseline conditions to 896/286 m^3/s (2050 SLR), and 1110/369 m^3/s (2100 SLR) (Fig. 7b). Tidal prism was strongly correlated with lateral velocity shear across the estuary mouth cross-section (Fig. 7c), with a linear regression yielding $R^2 = 0.91$ ($p < 0.001$), indicating that increases in tidal prism directly enhance flow velocities and mixing intensity, which promote tidal flushing of the estuaries. Correspondingly, modelled residence times for the Ribble decreased from a median of 2.79 days (baseline) to 1.29 days (2050 SLR) and 0.63 days (2100 SLR) (Fig. 7d), reductions of 53.8% and 77.4% respectively.

The future SLR scenarios showed that the variability in residence times (both inter-estuary variability due to volume/shape and temporal variability due to tidal/fluvial forcing) generally decreased from the baseline results (Fig. 8a-c). Median residence times across the 52 estuaries declined from 3.74 days (baseline) to 1.94 days (2100), with flow-driven variability falling from a median of 0.76 to 0.24 days. Tidal variability was more stable (median: 3.27 to 2.33 days), reflecting competing effects of SLR-driven tidal amplification and increased

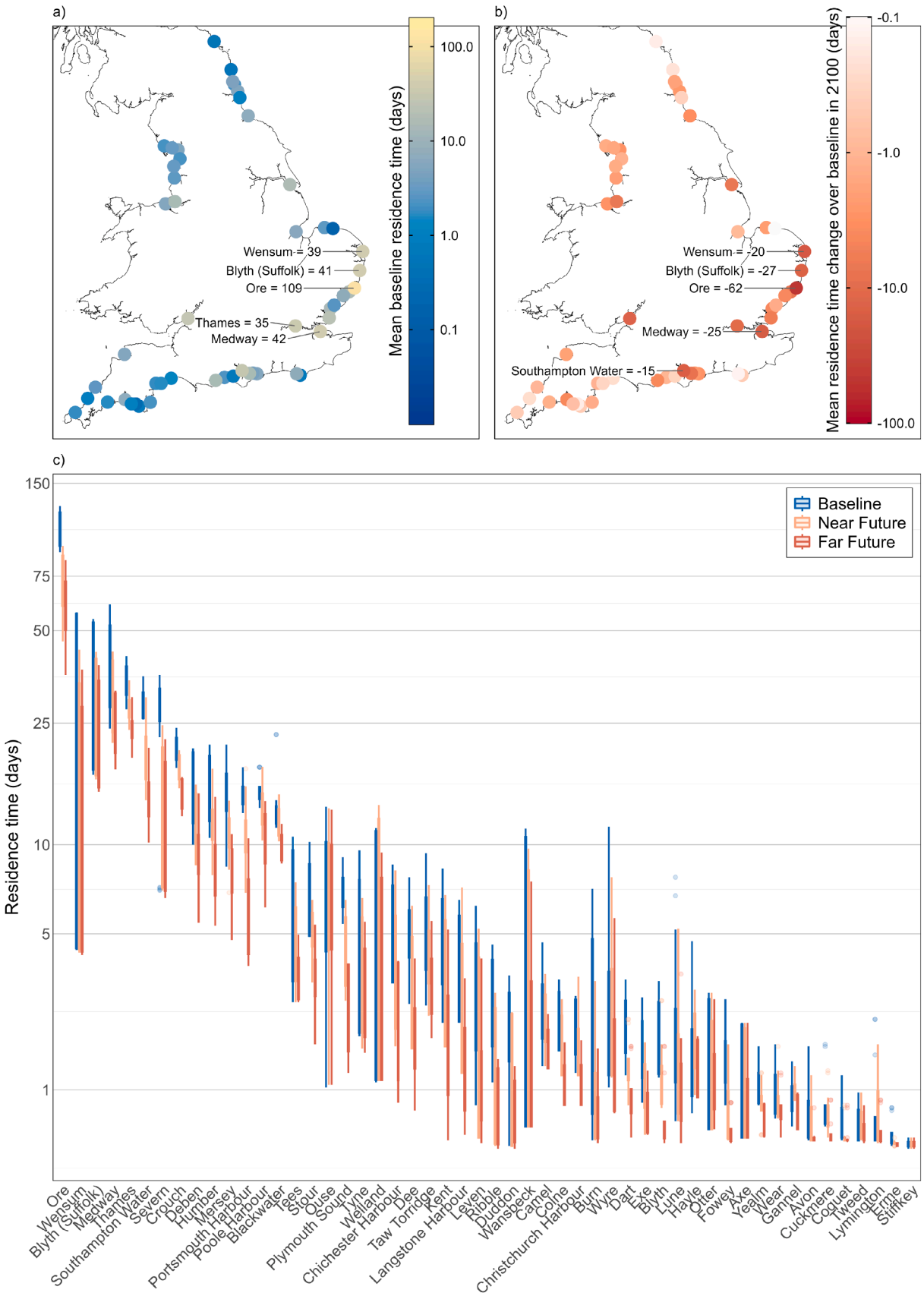


Fig. 6. (a) Mapped baseline (1980–2000) mean residence times (Q50, averaged across tidal release states), with the five longest labelled. (b) Mapped change in mean residence time by 2100, with the five largest reductions labelled. (c) Residence time distributions across all 52 estuaries ranked by baseline mean, under baseline (blue), near-future 2050 (orange), and far-future 2100 (red) scenarios; boxes show interquartile range across all tidal and flow scenarios, whiskers show full range, dots show outliers. Y-axis is log-scaled (days).

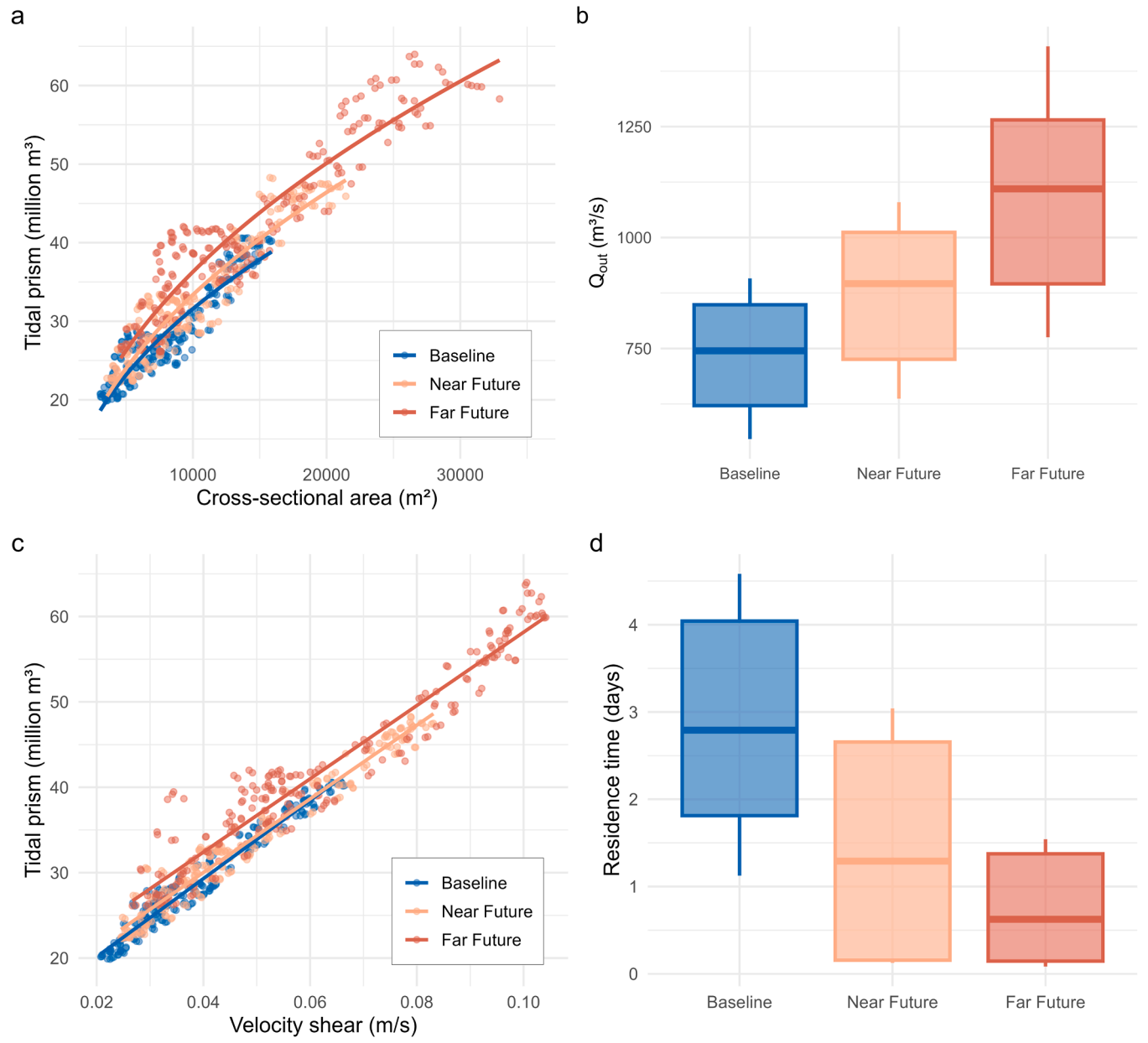


Fig. 7. Ribble estuary hydrodynamic metrics under baseline (blue), near-future 2050 (orange), and far-future 2100 (red) scenarios. (a) Tidal prism vs. mouth cross-sectional area with power-law fits. (b) Ebb discharge distributions. (c) Tidal prism vs. lateral velocity shear with linear regression fits. (d) Residence time distributions.

flushing.

The positive log-linear relationship between estuarine volume and residence time was statistically significant across all scenarios but weakened progressively under SLR: baseline ($r^2 = 0.360$, slope = 0.427, $p = 2.6 \times 10^{-6}$); 2050 SLR ($r^2 = 0.331$, slope = 0.416, $p = 8.2 \times 10^{-6}$); 2100 SLR ($r^2 = 0.286$, slope = 0.415, $p = 4.4 \times 10^{-5}$). By 2100, residence times ranged from 0.15 to 60.7 days (mean 6.33 days), representing a mean reduction of 4.48 days (45.5%) from baseline, whilst mean estuarine volumes increased by 22.4×10^6 m^3 (+35.9%; Fig. 8d). The largest reductions were in the Fowey, Ribble, Blyth, and Duddon, while the smallest were in the Ouse (−3.0%), Tweed (−8.6%), and Axe (−13.1%).

For the 2100 SLR simulations, most estuaries (n = 31; 60%) exhibited reductions in both flow-driven and tidal-driven temporal variability in residence times, including large systems such as the Severn, Mersey, and Blackwater (See Supplementary Figure S22). Flow-driven variability decreased in 46 estuaries, increased in 3, and 3 estuaries showed no change. Wensum experienced the greatest reduction (−23 days) and Poole Harbour showed the greatest increase (+0.25 days). Tidal-driven variability was more mixed: 35 estuaries showed reduced variability in residence times, 15 showed increases, and 2 showed no change. The Ore increased the most (+21.2 days) and the Blackwater decreased the most (−8.4 days).

14 estuaries showed a shift toward stronger tidal-dominance of residence time due to 2100 SLR (i.e., declining flow-driven variability but increasing tidal-driven variability), including the Humber, Blyth (Suffolk), and Deben. Conversely, three estuaries showed a shift towards fluvial dominance (Stour, Colne, and Christchurch Harbour). Only Poole Harbour showed increases in both drivers, while Stiffkey showed negligible tidal change but increased flow-driven variability.

The reduction in mean residence times due to 2100 SLR was compared to the baseline tide- and river-driven variability in residence times (See Supplementary Figure S23). In most estuaries, the baseline variability exceeded the SLR-driven change in mean residence times. However, there were four estuaries (Plymouth Sound, Portsmouth

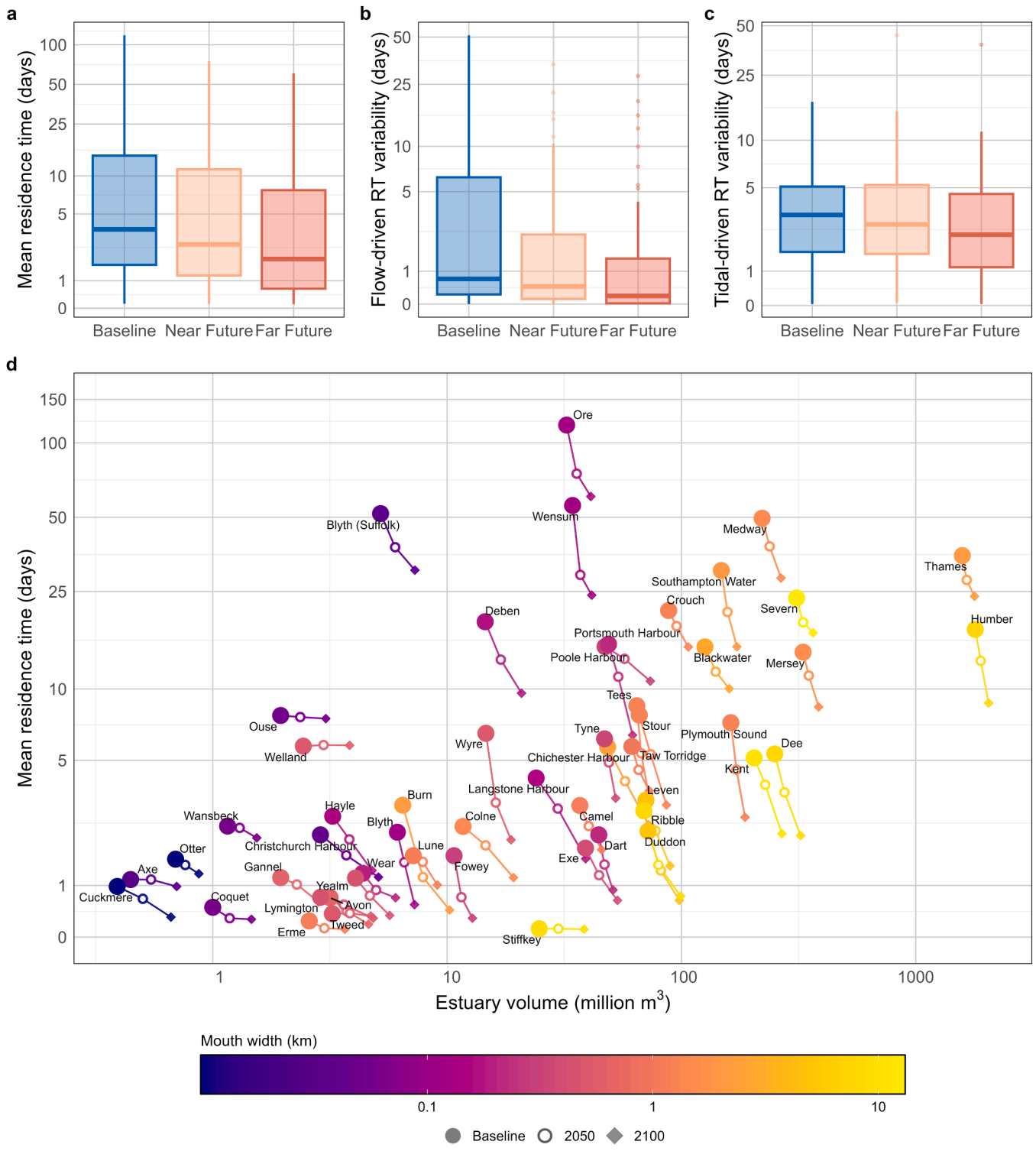


Fig. 8. (a–c) Distributions of mean residence time (Q50, averaged across tidal release states), flow-driven variability, and tidal-driven variability across all 52 estuaries under baseline, near-future 2050, and far-future 2100 SLR scenarios. (d) Estuary trajectories in volume–residence time space from baseline (circle) through 2050 (hollow circle) to 2100 (diamond), coloured by mouth width (km). Both axes are log-scaled.

Harbour, Southampton Water, and Ore) where the SLR-driven change in mean residence times exceeded the baseline variability, indicating a step-change in flushing behaviour. For example, in Plymouth Sound, the simulated 2100 SLR (+0.79 m) scenarios reduced the mean residence time by nearly five days compared to the baseline scenarios, which varied by 3.9 days due to tidal and river forcing. Across all estuaries, a positive relationship was apparent between baseline forcing-driven variability and the magnitude of the 2100 SLR-induced mean reduction ($R^2 = 0.65$, slope $= 0.53$, $p = 7.4 \times 10^{-13}$). This indicates that estuaries experiencing highly dynamic flushing variations under current conditions are structurally more sensitive to long-term shifts under SLR.

4. Discussion and conclusion

4.1. Quantification of estuarine residence times

This study has provided the first quantification of estuarine residence times across the majority (52) of English estuaries, under present-day and projected sea-level rise conditions. The hydrodynamic simulations of tracer-based dispersal were computed using validated, spatially high-resolution (e.g., built on newly developed 20 m DEMs designed to resolve estuarine morphological features; Barada et al., 2026, *in review*) Delft3D D-Flow (depth-averaged) and D-Water Quality modelling. These simulations provide accurate estimates of estuarine residence times under changing tidal and riverine conditions, as well as under projected (RCP8.5) 21st century sea-level rise. The simulations inherently included return flows and mixing of tracers once exported from the estuary. This provides a more accurate representation of estuarine renewal than traditional static flushing times derived directly from hydrodynamic exchange metrics (volumes, discharges, tidal prism), which do not account for return flow (e.g., Sheldon and Alber, 2006; Haddout et al., 2022). The approach improves upon static flushing time estimates that do include a return flow factor (e.g., Monsen et al., 2002), by simulating changes in hydrodynamic over a mean spring-neap tidal cycle.

The simulated baseline residence times for the Mersey (8.5–19.2 days) are longer than the 1–4 days reported by Yuan et al. (2007), likely reflecting differences in the modelling frameworks employed. The WFD polygon approach of this study covers a larger area than the averaging domain used by of Yuan et al. (Gladstone to Fiddlers Ferry; approx. 23% smaller area of analysis), capturing the slower flushing upper estuary consistent with Yuan et al.'s own local tracer releases which demonstrated residence times of up to 450 h (~19 days) in the upper estuary alone. Furthermore, the structured mesh employed in the 2007 study poorly resolves the Mersey's small scale hydrodynamic features whereas the unstructured mesh used here better represents intertidal channels and embayments that act as retention zones.

Under baseline conditions there was considerable intra-estuary variability in mean residence times due to differences in estuary volume and shape. Estuaries with larger volumes, such as the Humber, Severn, and Thames, exhibited longer residence times than estuaries with smaller volumes, such as the Cuckmere and Axe. For each estuary, there was also substantial temporal variability in residence times under different tidal/fluvial conditions. Estuaries with rapid flushing (e.g., Cuckmere, Erme, Lymington) were typically small, open-mouthed systems or characterised by relatively high freshwater inflow and tidal exchange, while those with the longest residence times (e.g., Ore, Wensum, Humber) exhibited either mesotidal or microtidal regimes, limited freshwater input, or large estuarine volume relative to exchange fluxes.

The Ore estuary has the longest baseline residence time, of between 89.8 and 126.8 days. Even though it is relatively small (volume = 32.4 million m^3), it is microtidal (spring tidal range = 1.9 m) and has low freshwater inputs (median river discharge = 0.14 m^3/s), characteristics which limit its capacity for effective flushing. Other estuaries with relatively long residence times (generally greater than two weeks) and similar shape characteristics included the Blyth (Suffolk), Wensum, Poole Harbour, Deben, and Portsmouth Harbour. These systems share common physical characteristics that limit effective estuarine flushing: microtidal regimes (tidal range <2 m) and low freshwater inputs (median river discharge <3 m^3/s). Whereas for Southampton Water, despite the estuary being shorter (~20 km) with a wide mouth cross-section, the mesotidal regime (tidal range of 2–4 m) limits the capacity of the tidal flux to flush the system. Combined with moderate freshwater inflow (median = 5.15 m^3/s), these factors result in extended travel paths and retention times for conservative tracers. Conversely, a subset of fast-response estuaries (i.e., systems with baseline residence times <1 day, n = 8) was also identified. These include the Cuckmere, Coquet, Tweed, Avon, Erme, Lymington, and Stiffkey. These estuaries are generally small in area (<2 km^2) and either possess high discharge-to-volume ratios (e.g., Lymington, ~15 m^3/s) or exhibit open mouth cross-sections and large tidal fluxes that promote rapid flushing. The majority of estuaries fell into an intermediate category, with 20 systems (38%) exhibiting median residence times between 2 and 8.25 days. Examples include the Ribble (2.79 days), Dee (5.17 days), Ouse (7.56 days), and Tees (8.25 days). These systems are typically of moderate size (10–70 km^2), with mesotidal ranges (2–4 m) and moderate freshwater inflows (5–25 m^3/s), resulting in flushing on the order of several days. Estuary morphologies characterised by open mouths and relatively direct axial pathways, promote more efficient exchange than long, narrow estuaries, yet their storage volumes are sufficiently large to prevent the rapid flushing observed in the smallest fast-response systems.

Our findings are consistent with recent global assessments that identify tidal prism, estuary geometry, and fluvial-tidal interactions as first-order controls on residence time and water quality vulnerability (de Abreu et al., 2020; Khojasteh et al., 2023). In tidally dominated systems – typically shallow, macrotidal or hypertidal, and possessing extensive intertidal areas – residence times varied by several days over the spring-neap cycle due to marked fluctuations in tidal range (Robins et al., 2015) and thus tidal prism. These dynamics are well documented, where spring-neap variation governs the effective tidal flushing volume (Khojasteh et al., 2021). In contrast, fluvially dominated systems exhibited stronger sensitivity to discharge variability, particularly under low-flow conditions where the river contribution to the estuarine volume becomes critical in regulating flushing times.

4.2. Implications for water quality and estuarine management

Previous modelling studies have linked changes in residence time to changes in nutrient dynamics, phytoplankton bloom potential, larval transport, and pathogen viability (Chen et al., 2015; van Maanen and Sottolichio, 2018). Shorter residence times enhance flushing and reduce the accumulation and persistence of nutrients, suspended sediments, and contaminants, thereby lowering the risk of eutrophication, harmful algal blooms, and hypoxia. For example, Defne & Ganju (2015) showed that estuarine sub-basins with faster turnover (flushing) exhibited lower potential for nutrient accumulation, while Hiatt et al. (2018) demonstrated that short exposure times reduce pollutant residence and limit water quality deterioration. Shorter retention also decreases the persistence of human pathogens and faecal indicator organisms, as rapid flushing limits the time available for microbial survival and accumulation in shellfish waters, reducing public health risks (Ralston et al., 2015; Clough et al., 2025). However, very fast flushing can constrain phytoplankton growth by limiting bloom development windows (Ralston et al., 2015) and can reduce larval retention, disrupting ecological connectivity (Shen et al., 2022). In contrast, longer residence times promote nutrient recycling, stratification, and sediment–nutrient interactions, creating conditions favourable to bloom formation, oxygen depletion, and human pathogen persistence (Hewageegana et al., 2023). These mechanisms are not purely theoretical for English estuaries. Southampton Water (identified as having a long baseline residence time driven by mesootidal regime and moderate freshwater input) is a well documented site of eutrophication and nutrient enrichment linked to limited flushing capacity (Nedwell et al., 2002). The residence time reductions projected here under SLR pathways therefore carry implications for the future nutrient retention and bloom risk within this estuary.

Residence times in this study varied by up to 51 days across tidal states and flow conditions within individual estuaries, meaning that the water quality risk associated with a given nutrient or pathogen loading event is highly dependent on prevailing hydrological conditions. During low-flow, neap-tide conditions, prolonged residence may promote stratification and nutrient accumulation, whereas spring-tide or high-discharge conditions in the same estuary may flush inputs before

bloom development can occur (Dodrill et al., 2023). Furthermore, estuaries with long residence times are inherently more sensitive to nutrient and contaminant loading (Shen et al., 2022) and may therefore require proportionally more stringent catchment management to achieve equivalent water quality outcomes. Conversely, estuaries with very short residence times may be less responsive to local management interventions.

A central finding of this study was the consistent reduction in estuarine residence times under projected SLR. This reduction was evident across all estuaries investigated and is primarily attributable to the increased tidal prism, which augments volumetric exchange between estuaries and coastal waters. Hydrodynamic analysis of the Ribble estuary showed that the tidal prism scaled near-proportionally with estuarine volume, yet the percentage increase in tidal prism exceeded that of volume across scenarios, highlighting enhanced tidal exchange as a dominant mechanism supporting reduced residence times under SLR. Estuaries with smaller intertidal areas (i.e., Wansbeck ~0.1 km^2 (Davidson et al., 1991)) or limited intertidal storage (i.e., Christchurch Harbour ~13,800 m^3 (ABPmer, 2025)) are less able to buffer these changes, showing weaker proportional increases in tidal prism under sea-level rise and thus smaller reductions in residence time than estuaries with large intertidal zones (Khojasteh et al., 2020). This behaviour is likely to be representative of many UK estuaries with extensive intertidal storage, where SLR drives disproportionate increases in tidal exchange relative to estuarine volume (Holleman and Stacey, 2014). The absence of any lengthening response reflects the physical characteristics of the studied estuaries rather than a general result: 51 of the 52 estuaries remained well-mixed under all flow scenarios (Section 2.1.3, Supplementary Table S3), so the stratification pathway by which SLR extends residence time in weakly tidal basins (i.e. Irby et al., 2018) does not apply here, while the potential for concurrent hydrological change to offset the SLR signal is considered in Section 4.3. This shift in dominant control from static volume to dynamic exchange capacity represents a key mechanism by which SLR will alter estuarine flushing behaviour in the future. This response aligns with findings from ensemble-based global modelling frameworks that demonstrate an amplification of tidal range and exchange potential under SLR scenarios, particularly in estuaries with narrowing geometry or reduced intertidal storage capacity (Sullivan et al., 2020; Khojasteh et al., 2021).

Our results suggest that under future SLR, although residence times generally decrease, estuaries with smaller intertidal areas may show less dramatic decreases, meaning that while flushing improves, some negative water-quality risks associated with slower residence (e.g. bloom potential, pathogen persistence) might persist longer in those systems. Notably, some estuaries demonstrated residence time reductions under SLR that exceeded the full range of variability caused by tidal and river flow fluctuations under present-day conditions (e.g., Plymouth Sound). Such shifts imply a fundamental reconfiguration of estuarine hydrodynamics and point to potential transformations in ecosystem function, biogeochemical cycling, and pollutant fate. Consequently, estuaries that demonstrate SLR-driven residence time changes beyond current variability thresholds should be considered priority systems for further climate-resilience and adaptation research.

4.3. Limitations and further research

Our simulations maintained temporally constant 5th/50th/95th percentile river flows across future time slices. The percentile-based approach was designed to characterise the envelope of residence time variability driven by hydrological forcing, rather than to reproduce any specific discharge timeseries (i.e. the 5th, 50th and 95th percentile flows bound the range of conditions each estuary is expected to experience. The Liverpool Bay validation (Supplementary Fig. S4) tested this envelope directly, forcing eight estuaries with realistic temporally variable (15-minute resolution) river flow data to simulate short-term hydrodynamic variability from rapidly changing freshwater pulses. The results demonstrated that these more realistic simulated residence time broadly fell within the range of residence times simulated with temporally constant river flow forcing, confirming the envelope is well constrained for short term flow variability. However, the validation period does not cover a full annual cycle (i.e. winter high flow and summer low flow regimes). Seasonal differences in discharge could shift the timing and magnitude of water quality risk windows in ways not resolved by this study and should be a priority in future studies. Further, we simulated depth-averaged hydrodynamics, assuming limited effects of estuarine stratification on residence times. Estuarine stratification can significantly influence residence times by suppressing vertical mixing and creating density-driven exchange flows that alter the effective flushing of dissolved constituents (Geyer and MacCready, 2014). In well-stratified systems, the depth-averaged approach adopted here may underestimate near-bed residence times, where dense saline water can remain largely isolated from the overlying freshwater layer, and overestimate residence times in the surface layer where buoyancy-driven outflow is concentrated (Kim et al., 2025). Model validation in this study relied on tidal elevation and salinity as hydrodynamic validation parameters yet only serve as indirect proxies of tracer transport and residence time. Future related studies should consider whether these assumptions are appropriate on an estuary specific basis.

The baseline temporally constant percentile river flows were also used across future SLR scenarios due to the absence of high-resolution projected flow data. Observed trends from regional hydrological analyses suggest that 5th percentile flows may decrease in future climates, while 95th percentile flows may increase (Lane et al., 2022; Kay, 2025), with these changes being highly spatially variable (Smith et al., 2024) – an outcome that would respectively increase or decrease residence times and modulate the net impact of SLR. Although these effects were not explicitly modelled, their implications can be inferred from future simulations (see Fig. 5, Fig. S15-S22) and suggest that SLR may not universally shorten residence time where concurrent drying trends reduce fluvial input.

Future studies should incorporate additional climate drivers and estuarine processes important for water quality assessments, including warming waters, marine heatwaves, nutrient enrichment, pollution, and pathogen loading. Recent work highlights the role of sea-surface temperature climate change extremes, with northeast England estuaries projected to warm fastest (>0.6 °C $decade^{-1}$; (Robins and Lyddon 2026) and the interactions between altered river discharge and storm surges, with the largest projected surge increases in northwest England (>0.03 m $decade^{-1}$; (Robins and Lyddon 2026) both of which are likely to exacerbate estuarine water quality risks under climate change. Bathymetry was held static across all SLR scenarios in this study, and morphological evolution was not represented. Morphological evolution and suspended sediment dynamics, such as the estuarine turbidity maximum and turbidity plumes that limit light penetration, will also be critical to capture (Winterwerp and Wang, 2013). With SLR, estuarine morphology is expected to adjust through intertidal loss, channel deepening, and landward migration (Pye and Blott, 2014; Townend et al., 2021). Modelling of UK estuaries suggests up to ~10% intertidal area loss and substantial widening and deepening of upper channels under a 1 m SLR scenario, altering tidal prism and storage capacity (Huthnance et al., 2007). Such morphological changes could present significant alterations to residence times relative to those presented in this study (i.e. intertidal loss and channel deepening could further increase tidal prism relative to a fixed bed, potentially amplifying the residence time reductions reported here, whereas sediment accretion keeping pace with SLR would dampen them. The results presented here should therefore be interpreted as the hydrodynamic response to SLR under present day bathymetry rather than a complete prediction of estuarine state in 2100. Episodic discharge behaviour should be better represented through high-resolution (e.g., hourly) projections of future river flows that include extreme flood and drought dynamics (Kay, 2022; Kay and Brown, 2023), which strongly influence estuarine

renewal and flushing. Coupled biogeochemical interactions, including algal bloom formation, sediment aggregation, and microbial/pathogen behaviour, require integration into model frameworks to reflect ecosystem responses more holistically (Khojasteh et al., 2021).

Furthermore, the employment of the simple tidal prism method substantially underestimated residence times compared to the Delft3D D-Water Quality outputs in the Ribble Estuary case study. Recent work by Robins and Lyddon (2026) demonstrated how the return flow factor, *b* (see Monsen et al., 2002), can be parameterised as a sigmoid function of tidal prism, calibrated against Delft3D outputs (see Supplementary section S5). This calibration enables the development of an expanded Estuary Box Model (EBM; Verri et al., 2021) that reproduces the variability in residence times across tidal and river flow conditions with far lower computational cost than using high-resolution hydrodynamic models. While Delft3D provides the most robust estimates of absolute residence times, the EBM framework allows the exploration of a much wider range of hydrodynamic and climate-forced scenarios, including hourly-scale variability in river flows and surges, that would be computationally prohibitive with Delft3D modelling.

Integrated hydrodynamic–biogeochemical models, such as Delft3D-WAQ, BLOOM, and D-Sediment Transport, will be essential for simulating the compound effects of episodic extremes and mean-state changes under future climate scenarios. Our hydrodynamic modelling of residence time provides a foundational step for this progression, establishing the physical basis needed to predict secondary water quality impacts such as harmful algal blooms, hypoxia, and pathogen dispersal and exposure risk (Clough et al., 2025).

4.4. Conclusions

This study demonstrates the transformative utility of spatially resolved hydrodynamic modelling to assess estuarine flushing dynamics across diverse morphological and hydrological settings. By producing high-resolution, standardised bathymetries for all major English estuaries, this study delivers a step-change in the capacity to simulate estuarine dynamics consistently at a national scale. Our results advance both conceptual understanding and predictive capacity by quantifying and reinforcing the importance of tidal prism, freshwater inflow, and estuarine geometry as controls on residence time and reveal SLR as a potentially dominant modifier of flushing dynamics in future decades. These findings emphasise the need to monitor and manage estuarine systems in a way that anticipates hydrodynamic shifts and their cascading effects on water quality, ecosystem health, and coastal resilience.

Data sources

Environment Agency (EA) (2015). WFD Transitional and Coastal Waterbodies Cycle 2 [Dataset]. Available at: https://www.data.gov.uk/dataset/3a75ec5f-a361–475c-80e3–52d93bbc5dbe/wfd-transitional-and-coastal-waterbodies-cycle-2 [Accessed 05/09/2024]. © Environment Agency copyright and/or database right 2015. All rights reserved.

Met Office (2018). UKCP18 sea level anomalies for marine projections around UK coastline (2007–2100) [dataset]. Available at: https://ukclimateprojections-ui.metoffice.gov.uk/products/MS4_Anomalies_Subset_01 [Accessed 07/07/2025].

Funding statement

This work was funded by the UK Department for Environment, Food and Rural Affairs (DEFRA) and the Environment Agency (EA) under the INVEST project. T.W.C., P.R., and **D.L.J.** were also funded through the BlueAdapt project, which received funding from the European Union's Horizon Europe research and innovation programme under grant agreementNo. 101057764 and by UKRI/HM Government. G.C. and L.D. were funded through the FUTURE-FLOOD project (NE/X014134/1). BGS engagement in this project was supported by BGS National Capability funding.

CRediT authorship contribution statement

Thomas W. Clough: Writing – review & editing, Writing – original draft, Visualization, Validation, Software, Methodology, Investigation, Formal analysis, Data curation, Conceptualization. **Charlotte Lyddon:** Writing – review & editing, Supervision, Resources, Project administration, Funding acquisition, Data curation, Conceptualization. **Aaron Furnish:** Writing – review & editing, Methodology, Investigation. **Mirko Barada:** Writing – review & editing, Methodology, Investigation. **Tom Coulthard:** Writing – review & editing, Supervision, Conceptualization. **Andy Barkwith:** Writing – review & editing, Supervision, Conceptualization. **Fai Fung:** Writing – review & editing, Supervision, Conceptualization. **Gemma Coxon:** Writing – review & editing, Supervision, Conceptualization. **Laura Devitt:** Writing – review & editing, Supervision, Conceptualization. **Davey L. Jones:** Writing – review & editing, Supervision, Project administration, Conceptualization. **Nick Hayes:** Writing – review & editing, Supervision, Project administration, Conceptualization. **Alec Hutchings:** Writing – review & editing, Supervision, Project administration, Conceptualization. **Harriet G. Orr:** Writing – review & editing, Supervision, Project administration, Conceptualization. **Peter Robins:** Writing – review & editing, Supervision, Project administration, Methodology, Investigation, Funding acquisition, Formal analysis, Data curation, Conceptualization.

Declaration of competing interest

The authors declare that they have no known competing financial interests or personal relationships that could have appeared to influence the work reported in this paper.

Acknowledgements

We thank colleagues from the British Geological Survey for their collaboration and engagement during INVEST, and the Met Office for provision of climate projection data and technical expertise. This paper is published with permission of the Director of the British Geological Survey. The views expressed are those of the authors and do not necessarily represent the views of the Environment Agency, the European Union, or other institutions.

Supplementary materials

Supplementary material associated with this article can be found, in the online version, at doi:10.1016/j.watres.2026.126999.

Data availability

Data will be made available on request.

References

ABPmer, 2025. New updates the UK Estuaries Database, adjusting data to align with water body boundaries used under the Water and Environment Regulations. In: ABPmer Report No. R.4802. A report produced by ABPmer for Environment Agency, March 2025.

Bai, J., Zhao, J., Zhang, Z., Tian, Z., 2022. Assessment and a review of research on surface water quality modeling. Ecol Modell. 466, 109888. https://doi.org/10.1016/j.ecolmodel.2022.109888.

Barada, M., Lyddon, C., Clough, T., Robins, P., 2026. Integrated high-resolution nationwide bathymetry of english estuaries. *Earth System Data Science* (*in review*).

Bianchi, T.S., 2007. Biogeochemistry of Estuaries. Oxford University Press.

Chen, W.B., Liu, W.C., Hsu, M.H., 2015. Modeling assessment of a saltwater intrusion and a transport time scale response to sea-level rise in a tidal estuary. Environ. Fluid Mech. 15, 491–514. https://doi.org/10.1007/s10652-014-9367-y.

Cloern, J.E., Jassby, A.D., 2010. Patterns and scales of phytoplankton variability in estuarine–coastal ecosystems. Estuaries and Coasts 33, 230–241. https://doi.org/10.1007/s12237-009-9195-3.
Clough, T.W., Silvester, R., Kevill, J., Malham, S.K., Cross, G., Robins, P., Jones, D.L., 2025. Predicting norovirus contamination and antimicrobial resistance in coastal waters from community and hospital-derived sources. Water Res. 288, 124555. https://doi.org/10.1016/j.watres.2025.124555.
Čož, N., Ahmadian, R. and Falconer, R., (2017). Modelling the impacts of marine renewable energy structures in the Severn Estuary and Bristol Channel, UK.
Davidson, N.C., Laffoley, D.D.A., Doody, J.P., Way, L.S., Gordon, J., Key, R.E., Drake, C. M., Pienkowski, M.W., Mitchell, R., Duff, K.L., 1991. Nature Conservation and Estuaries in Great Britain. Nature Conservancy Council, Peterborough, p. 422. https://doi.org/10.13140/2.1.3522.9448.
de Abreu, C.H., Barros, M.D.L.C., Brito, D.C., Teixeira, M.R., Cunha, A.C.D., 2020. Hydrodynamic modeling and simulation of water residence time in the estuary of the Lower Amazon River. Water (Basel). 12 (3), 660. https://doi.org/10.3390/w12030660.
Defne, Z., Ganju, N.K., 2015. Quantifying the residence time and flushing characteristics of a shallow, back-barrier estuary: application of hydrodynamic and particle tracking models. Estuaries and Coasts 38 (5), 1719–1734. https://doi.org/10.1007/s12237-014-9885-3.
Dodrill, T.N., Pan, Y., Peterson, T.D., 2023. River discharge mediates extent of phytoplankton and harmful algal bloom habitat in the Columbia river estuary (USA) during North Pacific marine heat waves. Estuaries and Coasts 46 (1), 166–181. https://doi.org/10.1007/s12237-022-01129-y.
Du, J., Shen, J., Zhang, Y.J., Ye, F., Liu, Z., Wang, Z., Wang, Y.P., Yu, X., Sisson, M., Wang, H.V., 2018. Tidal response to sea-level rise in different types of estuaries: the importance of length, bathymetry, and geometry. Geophys Res Lett. 45 (1), 227–235. https://doi.org/10.1002/2017GL075963.
Egbert, G.D., Bennett, A.F., Foreman, M.G., 1994. TOPEX/POSEIDON tides estimated using a global inverse model. J. Geophys. Res.: Oceans 99 (C12), 24821–24852.
Fischer, H.B., List, E.J., Koh, R.C.Y., Imberger, J., Brooks, N.H., 1979. Mixing in Inland and Coastal Waters. Academic Press, San Diego.
Geyer, W.R., MacCready, P., 2014. The estuarine circulation. Annu Rev Fluid Mech. 46 (1), 175–197. https://doi.org/10.1146/annurev-fluid-010313-141302.
Gillibrand, P.A., Inall, M.E., Portilla, E., Tett, P., 2013. A box model of the seasonal exchange and mixing in regions of restricted exchange: application to two contrasting Scottish inlets. Environ. Model. Softw. 43, 144–159. https://doi.org/10.1016/j.envsoft.2013.02.008.
Haddout, S., Priya, K.L., Ljubenkov, I., 2022. The calculation of estuarine flushing times in convergent estuaries using fresh-water fraction method. Int. J. River Basin Manag. 20 (1), 123–136. https://doi.org/10.1080/15715124.2020.1719121.
Hall, J.W., Sayers, P.B., Walkden, M.J., Panzeri, M., 2006. Impacts of climate change on coastal flood risk in England and Wales: 2030–2100. Philos. Trans. R. Soc., A. 364 (1841), 1027–1049. https://doi.org/10.1098/rsta.2006.1752.
Hewageegana, V.H., Olabarrieta, M., Gonzalez-Ondina, J.M., 2023. Main physical processes affecting the residence times of a micro-tidal estuary. J Mar Sci Eng. 11 (7), 1333. https://doi.org/10.3390/jmse11071333.
Hiatt, M., Castañeda-Moya, E., Twilley, R., Hodges, B.R., Passalacqua, P., 2018. Channel-island connectivity affects water exposure time distributions in a coastal river delta. Water Resour Res. 54 (3), 2212–2232. https://doi.org/10.1002/2017WR021289.
Holleman, R.C., Stacey, M.T., 2014. Coupling of sea level rise, tidal amplification, and inundation. J Phys Oceanogr. 44 (5), 1439–1455. https://doi.org/10.1175/JPO-D-13-0214.1.
Honti, M., Istvánovics, V., Kovács, Á.S., 2010. Balancing between retention and flushing in river networks—Optimizing nutrient management to improve trophic state. Sci. Total Environ. 408 (20), 4712–4721. https://doi.org/10.1016/j.scitotenv.2010.06.054.
Huggett, R.D., Purdie, D.A., Haigh, I.D., 2021. Modelling the influence of riverine inputs on the circulation and flushing times of small shallow estuaries. Estuar. Coast. 44 (1), 54–69. https://doi.org/10.1007/s12237-020-00776-3.
Huthnance, J.M., Karunarathna, G., Lane, A., Manning, A.J., Norton, P., Reeve, D., Spearman, J., Soulsby, R.L., Townend, I.H., Wright, A., 2007. Development of estuary morphological models. Flood Risk Assessment II.
Iglesias, I., Avilez-Valente, P., Pinho, J.L., Bio, A., Vieira, J.M.P., Bastos, L. and Veloso-Gomes, F., (2019). *Numerical modeling tools applied to estuarine and coastal hydrodynamics: a user perspective*. IntechOpen. https://doi.org/10.5772/intechopen.85521.
Irby, I.D., Friedrichs, M.A., Da, F., Hinson, K.E., 2018. The competing impacts of climate change and nutrient reductions on dissolved oxygen in Chesapeake Bay. Biogeosciences. 15 (9), 2649–2668. https://doi.org/10.5194/bg-15-2649-2018.
Jevrejeva, S., Williams, J., Vousdoukas, M.I., Jackson, L.P., 2023. Future sea level rise dominates changes in worst case extreme sea levels along the global coastline by 2100. Environ. Res. Lett. 18 (2), 024037. https://doi.org/10.1088/1748-9326/acb504.
Jiang, L., Gerkema, T., Idier, D., Slangen, A.B., Soetaert, K., 2020. Effects of sea-level rise on tides and sediment dynamics in a Dutch tidal bay. Ocean Science. 16 (2), 307–321. https://doi.org/10.5194/os-16-307-2020.
Kay, A., 2022. Differences in hydrological impacts using regional climate model and nested convection-permitting model data. Clim Change. 173 (1), 11. https://doi.org/10.1007/s10584-022-03405-z.
Kay, A.L., 2025. A comparison of hydrological impacts from two ensembles of regional climate projections with a range of climate sensitivities. Reg Environ Change. 25 (3), 89. https://doi.org/10.1007/s10113-025-02426-5.
Kay, A.L., Brown, M.J., 2023. Using sub-daily precipitation for grid-based hydrological modelling across Great Britain: assessing model performance and comparing flood impacts under climate change. J. Hydrol. Reg. Stud. 50, 101588. https://doi.org/10.1016/j.ejrh.2023.101588.
Kennish, M.J., 2002. Environmental threats and environmental future of estuaries. Environ Conserv. 29 (1), 78–107. https://doi.org/10.1017/S0376892902000061.
Kerl, C.F., Basallote, M.D., Käberich, M., Oldani, E., Espejo, N.P.C., Blanco, A.E.C., Cánovas, C.R., Nieto, J.M., Planer-Friedrich, B., 2023. Consequences of sea level rise for high metal (loid) loads in the Ría of Huelva estuary sediments. Sci. Total Environ. 873, 162354. https://doi.org/10.1016/j.scitotenv.2023.162354.
Khojasteh, D., Felder, S., Heimhuber, V., Glamore, W., 2023. A global assessment of estuarine tidal response to sea level rise. Sci. Total Environ. 894, 165011. https://doi.org/10.1016/j.scitotenv.2023.165011.
Khojasteh, D., Glamore, W., Heimhuber, V., Felder, S., 2021. Sea level rise impacts on estuarine dynamics: a review. Sci. Total Environ. 780, 146470. https://doi.org/10.1016/j.scitotenv.2021.146470.
Khojasteh, D., Hottinger, S., Felder, S., De Cesare, G., Heimhuber, V., Hanslow, D.J., Glamore, W., 2020. Estuarine tidal response to sea level rise: the significance of entrance restriction. Estuar Coast Shelf Sci. 244, 106941. https://doi.org/10.1016/j.ecss.2020.106941.
Kim, B.K., Kim, D.H., Hwang, J.H., 2025. Impact of water residence time and stratification on water quality improvement of an artificial brackish waterway. J. Hydrol. Reg. Stud. 57, 102091. https://doi.org/10.1016/j.ejrh.2024.102091.
Lane, R.A., Coxon, G., Freer, J., Seibert, J., Wagener, T., 2022. A large-sample investigation into uncertain climate change impacts on high flows across Great Britain. Hydrol. Earth. Syst. Sci. 26 (21), 5535–5554. https://doi.org/10.5194/hess-26-5535-2022.
Legg, S., 2021. IPCC, 2021: climate change 2021-the physical science basis. Interaction. 49 (4), 44–45.
Luketina, D., 1998. Simple tidal prism models revisited. Estuar Coast Shelf Sci 46 (1), 77–84. https://doi.org/10.1006/ecss.1997.0235.
Lyddon, C., Robins, P., Lewis, M., Barkwith, A., Vasilopoulos, G., Haigh, I., Coulthard, T., 2023. Historic spatial patterns of storm-driven compound events in UK estuaries. Estuaries and Coasts 46 (1), 30–56. https://doi.org/10.1007/s12237-022-01115-4.
MacCready, P., McCabe, R.M., Siedlecki, S.A., Lorenz, M., Giddings, S.N., Bos, J., Albertson, S., Banas, N.S., Garnier, S., 2021. Estuarine circulation, mixing, and residence times in the Salish Sea. J. Geophys. Res. Oceans. 126 (2), e2020JC016738. https://doi.org/10.1029/2020JC016738.
Mendes, J., Ruela, R., Picado, A., Pinheiro, J.P., Ribeiro, A.S., Pereira, H., Dias, J.M., 2021. Modeling dynamic processes of mondego estuary and óbidos lagoon using delft3D. J Mar Sci Eng. 9 (1), 91. https://doi.org/10.3390/jmse9010091.
Met Office, 2014. Winter storms, January to February 2014. Available at: https://weather.metoffice.gov.uk/binaries/content/assets/metofficegovuk/pdf/weather/learn-about/uk-past-events/interesting/2014/winter-storms-january-to-february-2014—met-office.pdf [Accessed 18/07/2025].
Monsen, N.E., Cloern, J.E., Lucas, L.V., Monismith, S.G., 2002. A comment on the use of flushing time, residence time, and age as transport time scales. Limnol. Oceanogr. 47 (5), 1545–1553. https://doi.org/10.4319/lo.2002.47.5.1545.
Mora-Uribe, N., Caamaño-Avendaño, D., Villagrán-Valenzuela, M., Roco-Videla, Á., Alcayaga, H., 2025. Trends and applications of hydro-morphological modeling in estuarine systems: a systematic review of the past 15 years. J Mar Sci Eng. 13 (6), 1056. https://doi.org/10.3390/jmse13061056.
Nedwell, D.B., Dong, L.F., Sage, A., Underwood, G.J.C., 2002. Variations of the nutrients loads to the mainland UK estuaries: correlation with catchment areas, urbanization and coastal eutrophication. Estuar Coast Shelf Sci. 54 (6), 951–970. https://doi.org/10.1006/ecss.2001.0867.
Nicholls, R.J., Cazenave, A., 2010. Sea-level rise and its impact on coastal zones. Science (1979) 328 (5985), 1517–1520. https://doi.org/10.1126/science.1185782.
Palmer, K., Watson, C., Fischer, A., 2019. Non-linear interactions between sea-level rise, tides, and geomorphic change in the Tamar Estuary, Australia. Estuar Coast Shelf Sci. 225, 106247. https://doi.org/10.1016/j.ecss.2019.106247.
Pannozzo, N., Leonardi, N., Carnacina, I., Smedley, R., 2021. Salt marsh resilience to sea-level rise and increased storm intensity. Geomorphology 389, 107825. https://doi.org/10.1016/j.geomorph.2021.107825.
Polton, J.A., Palmer, M.R., Howarth, M.J., 2011. Physical and dynamical oceanography of Liverpool Bay. Ocean Dyn. 61, 1421–1439. https://doi.org/10.1007/s10236-011-0431-6.
Pugh, D., Woodworth, P., 2014. Sea-level science: Understanding tides, surges, Tsunamis and Mean Sea-Level Changes. Cambridge University Press.
Pye, K., Blott, S.J., 2014. The geomorphology of UK estuaries: the role of geological controls, antecedent conditions and human activities. Estuar Coast Shelf Sci. 150, 196–214. https://doi.org/10.1016/j.ecss.2014.05.014.
Ralston, D.K., Brosnahan, M.L., Fox, S.E., Lee, K.D., Anderson, D.M., 2015. Temperature and residence time controls on an estuarine harmful algal bloom: modeling hydrodynamics and *alexandrium fundyense* in Nauset estuary. Estuaries and Coasts. 38 (6), 2240–2258. https://doi.org/10.1007/s12237-015-9949-z.
Ranjbar, M.H., Etemad-Shahidi, A., Kamranzad, B., 2020. Modeling the combined impact of climate change and sea-level rise on general circulation and residence time in a semi-enclosed sea. Sci. Total Environ. 740, 140073. https://doi.org/10.1016/j.scitotenv.2020.140073.
Robins, P.E., Neill, S.P., Lewis, M.J., Ward, S.L., 2015. Characterising the spatial and temporal variability of the tidal-stream energy resource over the northwest European shelf seas. Appl Energy. 147, 510–522. https://doi.org/10.1016/j.apenergy.2015.03.045.
Robins, P.E., Skov, M.W., Lewis, M.J., Giménez, L., Davies, A.G., Malham, S.K., Neill, S. P., McDonald, J.E., Whitton, T.A., Jackson, S.E., Jago, C.F., 2016. Impact of climate change on UK estuaries: a review of past trends and potential projections. Estuar Coast Shelf Sci. 169, 119–135. https://doi.org/10.1016/j.ecss.2015.12.016.

Robins, P. and Lyddon, C., 2026. INVEST: investigating the vulnerability of estuarine water quality to climate change.
Scafetta, N., 2024. Impacts and risks of "realistic" global warming projections for the 21st century. Geosci. Front. 15 (2), 101774. https://doi.org/10.1016/j.gsf.2023.101774.
Sheldon, J.E., Alber, M., 2006. The calculation of estuarine turnover times using freshwater fraction and tidal prism models: a critical evaluation. Estuaries and Coasts 29 (1), 133–146. https://doi.org/10.1007/BF02784705.
Shen, J., Du, J., Lucas, L.V., 2022. Simple relationships between residence time and annual nutrient retention, export, and loading for estuaries. Limnol. Oceanogr. 67 (4), 918–933. https://doi.org/10.1002/lno.12045.
Smith, B.A., Birkinshaw, S.J., Lewis, E., McGrady, E., Sayers, P., 2024. Physically-based modelling of UK river flows under climate change. Front. Water. 6, 1468855. https://doi.org/10.3389/frwa.2024.1468855.
Sullivan, J.C., Wan, Y., Willis, R.A., 2020. Modeling floodplain inundation, circulation, and residence time under changing tide and sea levels. Estuaries and Coasts 43 (4), 693–707. https://doi.org/10.1007/s12237-020-00709-0.
Townend, I., Zhou, Z., Guo, L., Coco, G., 2021. A morphological investigation of marine transgression in estuaries. Earth. Surf. Process. Landf. 46 (3), 626–641. https://doi.org/10.1002/esp.5050.
Valle-Levinson, A., 2010. Contemporary Issues in Estuarine Physics. Cambridge University Press.
Van Gent, M.R., 2014. Overview of physical modelling at Deltares, including the new Delta flume. In: Proceedings of the 5th Conference on the Application of Physical Modelling to Port and Coastal Protection. Orewa, New Zealand (Vol. 29).
van Maanen, B., Sottolichio, A., 2018. Hydro-and sediment dynamics in the Gironde estuary (France): sensitivity to seasonal variations in river inflow and sea level rise. Cont Shelf Res. 165, 37–50. https://doi.org/10.1016/j.csr.2018.06.001.
Vermeulen, T.J., 2003. Sensitivity analysis of fine sediment transport in the Humber estuary. In: Delft University of Technology & WL| delft hydraulics, MSc-thesis.
Verri, G., Mahmoudi Kurdistani, S., Coppini, G., Valentini, A., 2021. Recent advances of a box model to represent the estuarine dynamics: time-variable estuary length and eddy diffusivity. J. Adv. Model. Earth. Syst. 13 (4), e2020MS002276. https://doi.org/10.1029/2020MS002276.
Wang, J., Dai, Z., Fagherazzi, S., Zhang, X., Liu, X., 2022. Hydro-morphodynamics triggered by extreme riverine floods in a mega fluvial-tidal delta. Sci. Total Environ. 809, 152076. https://doi.org/10.1016/j.scitotenv.2021.152076.
Winterwerp, J.C., Wang, Z.B., 2013. Man-induced regime shifts in small estuaries—I: theory. Ocean Dyn. 63 (11), 1279–1292. https://doi.org/10.1007/s10236-013-0662-9.
Yang, Y., Guan, W., Deleersnijder, E., He, Z., 2022. Hydrodynamic and sediment transport modelling in the Pearl River Estuary and adjacent Chinese coastal zone during Typhoon Mangkhut. Cont Shelf Res. 233, 104645. https://doi.org/10.1016/j.csr.2022.104645.
Yuan, D., Lin, B., Falconer, R.A., 2007. A modelling study of residence time in a macro-tidal estuary. Estuar Coast Shelf Sci. 71 (3-4), 401–411. https://doi.org/10.1016/j.ecss.2006.08.023.
Zimmerman, J.T.F., 1976. Mixing and flushing of tidal embayments in the western dutch Wadden Sea part I: distribution of salinity and calculation of mixing time scales. Neth. J. Sea Res. 10 (2), 149–191. https://doi.org/10.1016/0077-7579(76)90013-2.
Zimmerman, J.T.F., 2018. Estuarine residence times. Hydrodynamics of Estuaries. CRC Press, pp. 75–84.